Establishment of a Human Corneal Epithelial Cell Line Lacking the Functional TACSTD2 Gene as an In Vitro Model for Gelatinous Drop-Like Dystrophy

Koji Kitazawa,[1] Satoshi Kawasaki,[1] Katsuhiko Shinomiya,[1] Keita Aoi,[1] Akira Matsuda,[2] Toshinari Funaki,[2] Kenta Yamasaki,[3] Mina Nakatsukasa,[1] Nobuyuki Ebihara,[2] Akira Murakami,[2] Junji Hamuro,[1] and Shigeru Kinoshita[1]

[1]Department of Ophthalmology, Kyoto Prefectural University of Medicine, Kyoto, Japan
[2]Department of Ophthalmology, Juntendo University School of Medicine, Tokyo, Japan
[3]Department of Biomedical Engineering, Faculty of Life and Medical Sciences, Doshisha University, Kyotanabe, Japan

Correspondence: Satoshi Kawasaki, Department of Ophthalmology, Kyoto Prefectural University of Medicine, 465 Kajii-cho, Hirokoji-agaru, Kawaramachi-dori, Kamigyo-ku, Kyoto 602-0841, Japan; bluenova@koto.kpu-m.ac.jp.

Submitted: September 28, 2012
Accepted: July 10, 2013

Citation: Kitazawa K, Kawasaki S, Shinomiya K, et al. Establishment of a human corneal epithelial cell line lacking the functional TACSTD2 gene as an in vitro model for gelatinous drop-like dystrophy. *Invest Ophthalmol Vis Sci.* 2013;54:5701-5711. DOI:10.1167/iovs.12-11043

Purpose. Gelatinous drop-like corneal dystrophy (GDLD) is characterized by subepithelial amyloid deposition that engenders severe vision loss. The exact mechanism of this disease has yet to be elucidated. No fundamental treatment exists. This study was conducted to establish an immortalized corneal epithelial cell line to be used as a GDLD disease model.

Methods. A corneal tissue specimen was obtained from a GDLD patient during surgery. Corneal epithelial cells were enzymatically separated from the cornea and were dissociated further into single cells. The epithelial cells were immortalized by the lentiviral transduction of the simian virus 40 (SV40) large T antigen and human telomerase reverse transcriptase (hTERT) genes. For the immortalized cells, proliferative kinetics, gene expressions, and functional analyses were performed.

Results. The immortalized corneal epithelial cells continued to proliferate despite cumulative population doubling that exceeded 100. The cells showed almost no sign of senescence and displayed strong colony-forming activity. The cells exhibited a low epithelial barrier function as well as decreased expression of tight-junction-related proteins claudin 1 and 7. Using the immortalized corneal epithelial cells derived from a GDLD patient, we tested the possibility of gene therapy.

Conclusions. We established an immortalized corneal epithelial cell line from a GDLD patient. The immortalized cells exhibited cellular phenotypes similar to those of in vivo GDLD. The immortalized cells are thought to be useful for the development of new therapies for treating GDLD corneas and for elucidation of the pathophysiology of GDLD.

Keywords: corneal dystrophy, gelatinous drop-like, immortalized cells

Gelatinous drop-like dystrophy (GDLD; OMIM #204870), which was first reported by Nakaizumi in 1914,[1] is characterized by amyloid deposition at the subepithelial region of the corneal stroma. The symptoms of GDLD patients, including severe photophobia, foreign-body sensation, and epiphora, usually appear in the first decade of life and engender blurred vision in late stages.[2-4] Reduction of the corneal epithelial barrier function and the resultant tear-fluid permeation into the corneal stroma are probably the primary pathologic events related to GDLD. However, the exact mechanism for the amyloid deposition remains unclear. GDLD is an inheritable disease with an autosomal recessive trait. It has been reported predominantly in Japan, with an estimated frequency of incidence of 1 in 30,000,[5,6] although it is extremely rare in the Western world, accounting for only a few reported cases to date.[2] The gene responsible for GDLD, discovered using linkage analysis and a candidate gene approach in 1999, was designated as tumor-associated calcium signal transducer 2 (TACSTD2) gene.[7,8]

GDLD appears to be an extremely refractory corneal disease. Several treatment remedies have been performed for GDLD-afflicted corneas such as penetrating or lamellar keratoplasty, laser photoablation, keratoprosthesis, and scraping of the abnormal subepithelial deposition.[9-11] However, in most GDLD patients, the disease symptoms generally recur within a few years after such interventions, thereby necessitating repeated keratoplasties.[12-14] No currently used treatment for GDLD is fundamental. All are merely supportive, aimed at providing temporary relief from disease symptoms. Disease models provide large amounts of invaluable information for the development of novel effective treatments. Wang et al. generated TACSTD2$^{-/-}$ mice as an animal model for GDLD. However, they described no apparent abnormality in the corneas of those mice.[15]

The TACSTD2 gene encodes a membrane glycoprotein[16] that transduces calcium signals as a cell surface receptor.[17] The TACSTD2 protein is expressed in normal epithelial cells of various types, such as those of the conjunctiva, skin, pharynx, esophagus, uterine cervix, and vagina.[18] In several epithelial tumor types, this often overexpressed protein has been regarded as playing a major role in tumorigenesis.[16,19] We have reported that the TACSTD2 protein is necessary for the

epithelial barrier function of corneal epithelium through binding to CLDN1 and CLDN7 proteins.[18] Numerous mutations have been reported for this gene, two-thirds of which are nonsense or frameshift mutations.[20,21] Such mutations might cause the truncation of the TACSTD2 protein, which engenders the defect of a C-terminal transmembrane domain, eventually leading to the loss of function of the gene.

In this study, we established an immortalized human corneal epithelial cell line lacking the functional TACSTD2 gene for use as an in vitro model of the GDLD cornea. The cells were created by the lentiviral transduction of the simian virus 40 (SV40) large T antigen and human telomerase reverse transcriptase (hTERT) genes to corneal epithelial cells of a GDLD patient. The cells showed markedly lower epithelial barrier function as well as decreased expression of the tight-junction–related proteins claudin (CLDN) 1 and 7, which is consistent with our previous findings related to in vivo GDLD corneas. The cells are expected to be useful for developing novel effective treatments for GDLD corneas and for elucidating the pathophysiology of the disease.

Materials and Methods

Ethical Issues

Prior informed consent in accordance with the Declaration of Helsinki was obtained from the GDLD patient. All experimental procedures were approved by the Institutional Review Board for human studies of Kyoto Prefectural University of Medicine (C-1067).

Antibodies

All antibodies were raised against human antigens (Table 1).

Oligomers

All oligomers used for this study were synthesized by Life Technologies Corp. (Carlsbad, CA) (Table 2).

Abbreviations

The immortalized corneal epithelial cell line from the GDLD patient and the immortalized corneal epithelial cell line from a normal cornea are abbreviated, respectively, herein as imHCE_GDLD and imHCE_normal.

Culture of Human Corneal Epithelial Cells Derived From Normal and GDLD Corneal Tissue Specimen

A 59-year-old Japanese woman bearing a biallelic loss-of-function mutation of the TACSTD2 gene (p.Gln118X) underwent lamellar keratoplasty and keratoepithelioplasty. A specimen of her corneal tissue was obtained at the time of surgery. A normal corneal tissue specimen was taken from a cornea intended for research obtained from Northwest Lyons Eye Bank (Seattle, WA).

Corneal epithelial sheets were peeled from these two corneas via the application of 1000 protease units (PU)/mL of dispase (Dispase type II; Godo Shusei Co., Ltd., Tokyo, Japan) at 4°C overnight. The peeled epithelial sheets were then dissociated via the application of trypsin-like protease (TrypLE Express; Life Technologies Corp.) at 37°C for 5 minutes. The dissociated corneal epithelial cells were seeded on a collagen-coated six-well plate and were cultured in a supplemented corneal epithelial cell-oriented growth medium (CnT-20; Cellntec Advanced Cell System AG, Bern, Switzerland) under standard culture conditions.

Lentiviral Vector Construction and Transduction of SV40 Large T Antigen and hTERT Genes

The coding sequences of SV40 large T antigen and hTERT genes were amplified by PCR and were TA-cloned into a commercial lentiviral vector (pLenti6.3_V5-TOPO; Life Technologies Corp.) (Figs. 1A, 1B). The lentiviral vectors were transfected to 293T cells along with three packaging plasmids (pLP1, pLP2, and pLP/glycoprotein of the vesicular stomatitis virus; Life Technologies Corp.) using a commercial transfection reagent (Fugene HD; Promega Corp., Madison, WI). After 48 hours of transfection, the supernatant of the culture medium was harvested, centrifuged briefly, and stored in a freezer at −80°C. For lentiviral transduction, the virus-containing supernatant was added to the cultures of the dissociated corneal epithelial cells in the presence of 5 μg/mL polybrene.

Population-Doubling (PD) Analysis

Growth kinetics were measured using PD analysis, as described previously.[22] Briefly, cells (5×10^4 to 1×10^5) were seeded to a T-25 plastic flask and were then fed every other day. When the cells reached subconfluence (approximately 70% confluence), they were harvested using TrypLE Express, counted, and seeded again to a new T25 plastic flask. Increment PD per passage was calculated with a formula $\log_2$ (Ch/Cs), where Ch corresponds to the number of harvested cells, and Cs corresponds to the number of seeded cells.

Colony-Forming Assay

Colony-forming activity was investigated as described in a previous report.[23] Briefly, single-cell suspensions of the transduced or nontransduced cells were seeded at a density of 1×10^2, 1×10^3, or 1×10^4 cells per well on a six-well plate in the presence of Mitomycin C–treated feeder cells and allowed to grow for 7 to 10 days. The cells were then fixed with 10% buffered formalin for 10 minutes, stained with 1% rhodamine B solution for 10 minutes, washed, and photographed.

Senescence-Associated β-Galactosidase (SAβgal) Assay

SA-βgal activity was detected using a commercially available kit (Senescence Detection Kit; Bio Vision, Inc., San Francisco, CA). Briefly, the cells were fixed and then stained with a staining solution (containing 5-bromo-4-chloro-3-indolyl-β-D-galactoside [X-gal]), included with the kit, at 37°C overnight. Then, they were photographed.

Telomere Repeat Amplification Protocol (TRAP) Assay

TRAP assay was performed according to a previous report, but with minor modifications.[24] Briefly, 2×10^5 cells were lysed. Telomerase substrate (TS) primer was elongated by the telomerase activity contained in the lysate. After purification, the reaction mixture was amplified by PCR using a 344 nM primer pair (TS primer and CX primer). The PCR products were then electrophoresed on a 10% nondenaturing acrylamide gel, stained (SYBR Green I; Takara Bio, Inc., Otsu, Japan), and photographed.

Immunostaining Analysis

Cells grown on a commercially available culture-glass slide (Nunc Lab-Tek Chamber Slide System; Thermo Fisher Scientif-

Investigative Ophthalmology & Visual Science

TABLE 1. List of Antibodies Used for This Study

Antibody	Category	Company*	Clone/Cat No.	Dilution
CLDN1	MM	Abnova	1C5-D9	×200
CLDN4	MM	Life Technologies	3E2C1	×100
CLDN7	MM	Life Technologies	5D10F3	×100
TACSTD2	GP	R&D	AF650	×100
OCLN	GP	Santa Cruz	sc-8145	×50
ZO-1	MM	Life Technologies	ZO1-1A12	×200
SV40 large T	MM	Abcam	PAb416	×100
hTERT	MM	Novocastra	44F12	×50

Cat, catalog; MM, mouse monoclonal; GP, goat polyclonal.

* Abnova, Abnova Corp., Taipei, Taiwan; Life Technologies, Life Technologies Corp., Carlsbad, CA; R&D, R&D Systems, Minneapolis, MN; Santa Cruz, Santa Cruz Biotechnology, Inc., Dallas, TX; Abcam, Abcam plc., Cambridge, UK; Novocastra, Novocastra Laboratories Ltd., Newcastle upon Tyne, UK.

ic, Inc., Rochester, NY) were fixed with Zamboni's fixative (phosphate-buffered combination of picric acid and paraformaldehyde) or 95% ice-cold ethanol, blocked with 1% skim milk, incubated overnight with a primary antibody at 4°C, washed with PBS, and incubated with a secondary antibody (Alexa Fluor 488-labeled anti-mouse or anti-goat IgG; Life Technologies Corp.) at room temperature for 1 hour. Subsequently, they were washed again with PBS, counterstained, mounted, covered with coverslips, and photographed using a fluorescence microscope (AX70 TRF; Olympus Corp., Tokyo, Japan) and a confocal laser scanning microscope (TCS-P2; Leica Microsystems, Wetzlar, Germany).

Western Blotting Analysis

Proteins were separated on a commercially available 4% to 20% gradient SDS-polyacrylamide gel (Mini-PROTEAN TGX; Bio-Rad Laboratories, Inc., Hercules, CA) and were transferred to a polyvinylidene difluoride membrane (Trans-Blot Turbo Transfer Pack; Bio-Rad Laboratories, Inc.). The blotted membrane was then blocked in TBS-T (Tris-buffered saline with 0.05% Tween 20) buffer containing 1% skim milk, incubated overnight with primary antibodies at 4°C, washed, incubated with a horseradish peroxidase–conjugated secondary antibody at room temperature for 1 hour, and washed again. A chemiluminescent reagent (ECL Advance Western Blotting Detection Kit; GE Healthcare, Little Chalfont, UK) was then applied onto the blotted membrane. The luminescent signal was detected using a chilled charge-coupled device (CCD) digital imaging camera (LAS-3000UVmini; Fujifilm Corp., Tokyo, Japan).

Reverse Transcription Polymerase Chain Reaction (RT-PCR)

RNA was reverse transcribed using a commercial reverse transcriptase (Superscript III; Life Technologies Corp.). The cDNA was amplified by PCR and then electrophoresed on a 2% agarose gel.

Measurement of Trans-Epithelial Resistance (TER)

Epithelial cells were cultured on 12-well porous membrane filters (Transwell, 0.4 μm pore; Corning, Inc., Corning, NY). Two days after the cells had reached 100% confluence, the culture medium was switched to a serum-containing, high-calcium medium (1 mM) to promote epithelial barrier formation. Resistance between the upper and lower chambers of the porous filter was measured using a volt-ohm meter (EVOM; World Precision Instruments, Sarasota, FL). The TER was then calculated by multiplying the measured resistance (ohms) by the culturing area of the filter (1.12 cm^2).

RESULTS

Characteristics of the Established Corneal Epithelial Cell Line From the GDLD Patient

The immortalized corneal epithelial cell line from the GDLD patient (imHCE_GDLD) exhibited a small, square, cell shape (Fig. 2A). When the cells reached confluence, they demonstrated an organized cobblestone-like appearance that is typical of epithelial-type cells. That cell shape resembled that of the immortalized corneal epithelial cell line from the normal cornea (imHCE_normal). The imHCE_GDLD cells were found to be completely devoid of the TACSTD2 protein, as judged from immunostaining analysis (Fig. 2B), although the cells did express the TACSTD2 gene at the RNA level (Fig. 2C). The expressed TACSTD2 mRNA was found to harbor the p.Gln118X mutation (Fig. 2D). We initially hypothesized that this discrepancy was attributable to the inability of the antibody to react to the truncated TACSTD2 protein produced by the nonsense mutation of the gene at the upstream region of its transmembrane domain. However, results showed that

TABLE 2. List of Oligomers Used for This Study

Primer	Sequence
SV40 large T_forward	5′-GGCGCCATGGATAAAGTTTTAAACAGAGAGGA-3′
SV40 large T_reverse	5′-TTATGTTTCAGGTTCAGGGGGAG-3′
hTERT_forward	5′-AGCAGGCACCATGCCGCGCGCTCC-3′
hTERT_reverse	5′-GCTGGGTTCTAGTCCAGGATGGTC-3′
TACSTD2_forward	5′-CTGACCTCCAAGTGTCTGCTG-3′
TACSTD2_reverse	5′-GTCCAGGTCTGAGTGGTTGAAG-3′
TS	5′-AATCCGTCGAGCAGAGTT-3′
CX	5′-CCCTTACCCTTACCC TTACCCTAA-3′

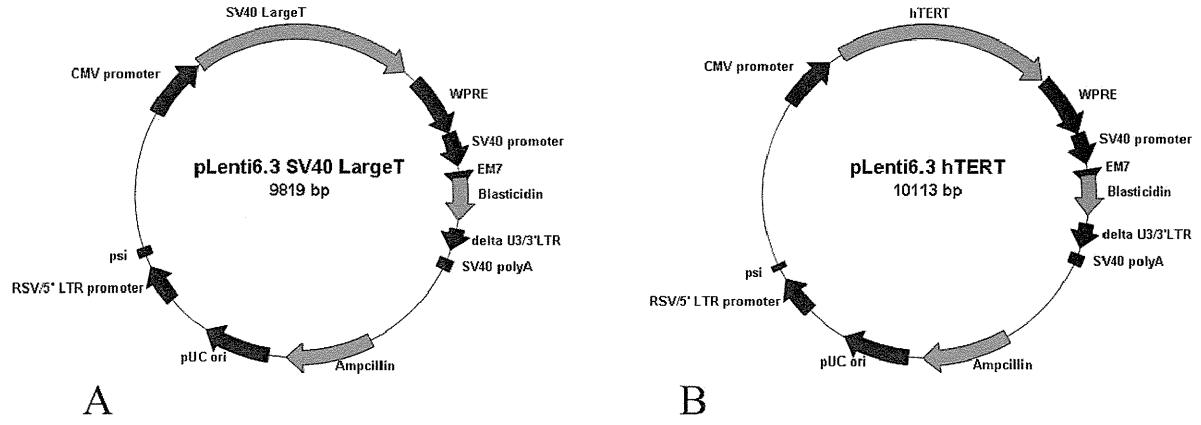

FIGURE 1. Schematic representation of the structure of lentivirus vectors expressing the SV40 large T antigen (**A**) and the hTERT genes (**B**).

the goat polyclonal antibody can recognize the TACSTD2 protein with the p.Gln118X nonsense mutation (Supplementary Fig. S1). Therefore, our current hypothesis is that the TACSTD2 protein with the p.Gln118X mutation is secreted to the extracellular space or is degraded within the cells. The imHCE_GDLD cells were found to express the SV40 large T antigen and hTERT genes (Figs. 2E, 2F), indicating that our lentiviral transduction process is efficient.

Cell Proliferative Kinetics, Senescent Status, Telomerase Activity, and Colony-Forming Activity in the Immortalized Corneal Epithelial Cell Line From the GDLD Patient

The cell proliferative kinetics was investigated using PD analysis (Fig. 3A). The imHCE_GDLD cells continued to proliferate after the cumulative PDs exceeded 104.7, although the nontransduced corneal epithelial cells from the GDLD patient stopped proliferating when the cumulative PDs reached 19.7.

Although their cumulative PDs exceeded 100, the imHCE_GDLD cells were rectangular and small (Fig. 3B). The nontransduced corneal epithelial cells from the GDLD patient exhibited almost identical cell shape and cell size to those of the imHCE_GDLD cells in their early stage of culture, but they gradually became more flattened and larger as their cumulative PDs increased. Their flattened cell shape appeared to be typical of senesced cells. Therefore, we tested the cellular senescent status by evaluating the SA-βgal activity. As depicted in Figure 3B, most nontransduced corneal epithelial cells from the GDLD patient exhibited blue staining in their cytoplasmic area when their cumulative PDs were 19.4. However, the imHCE_GDLD cells exhibited nearly unstained clear cell bodies, although some cells were stained faintly in blue when their cumulative PD was 54.1. Those results indicate clearly that the imHCE_GDLD cells were almost completely out of the senescent stage, irrespective of their PDs, although the nontransduced corneal epithelial cells from the GDLD patient entered the senescent stage as their PDs increased.

We regarded it as important to confirm whether the imHCE_GDLD cells acquired telomerase activity because the telomerase is a holoenzyme comprising proteins (dyskerin; DKC1 and telomerase protein component 1; TEP1)[25,26] and RNA (telomerase RNA component; TERC).[27] Therefore, the forced expression of the hTERT gene does not necessarily guarantee the acquisition of telomerase activity. The imHCE_GDLD cells showed clear laddering of the multiple-sized TRAP products (Fig. 3C). The intensity and the degree of extension to long fragments in the TRAP ladder of the imHCE_GDLD cells were at almost the same level as those of HeLa cells (well-known cancer cells that have been maintained continuously for more than 60 years)[28] and HCE-T cells (commonly used immortalized corneal epithelial cells established more than 20 years ago that have passed for many years).[29] Those results indicate that the forcedly expressed hTERT protein, which was expressed also under the regulation of inauthentic virus-origin promoter (cytomegalovirus promoter), integrated into a functionally competent telomerase complex and elongated the telomeric sequence of the chromosomal ends.

We also performed a colony-forming assay to examine the cell-proliferation competence of the imHCE_GDLD cells expanded from single cells. The imHCE_GDLD cells produced multiple-cell expansion foci that were larger and more numerous than the nontransduced corneal epithelial cells from the GDLD patient (Fig. 3D). The results strongly suggest that the imHCE_GDLD cells can be maintained for a much longer period.

Epithelial Barrier Function and Expression of Tight-Junction–Related Proteins in the imHCE_GDLD Cells

We next investigated whether the imHCE_GDLD cells had appropriate cellular features to be used as an in vitro model of a GDLD cornea. We initially investigated the epithelial barrier function of the imHCE_GDLD cells by measuring the TER. As portrayed in Figure 4A, the epithelial barrier function of the imHCE_GDLD cells was significantly lower than that of the imHCE_normal cells ($P < 0.05$, Student's t-test). We also investigated the expression of the tight-junction-related proteins in the imHCE_GDLD cells. The CLDN1 and CLDN7 protein expression levels were found to be reduced significantly more in the imHCE_GDLD cells than in the imHCE_normal cells (Fig. 4B), which is consistent with our earlier observation that the expression level of these proteins was decreased significantly in an in vivo GDLD cornea.[18] In addition, the immunostaining pattern of the CLDN1 and CLDN7 proteins was dramatically different from that in the imHCE_normal cells. The other three tight-junction-related proteins including CLDN4, occludin (OCLN), and zonula occludens-1 (ZO-1) were expressed both in the imHCE_GDLD and the imHCE_normal cells at an

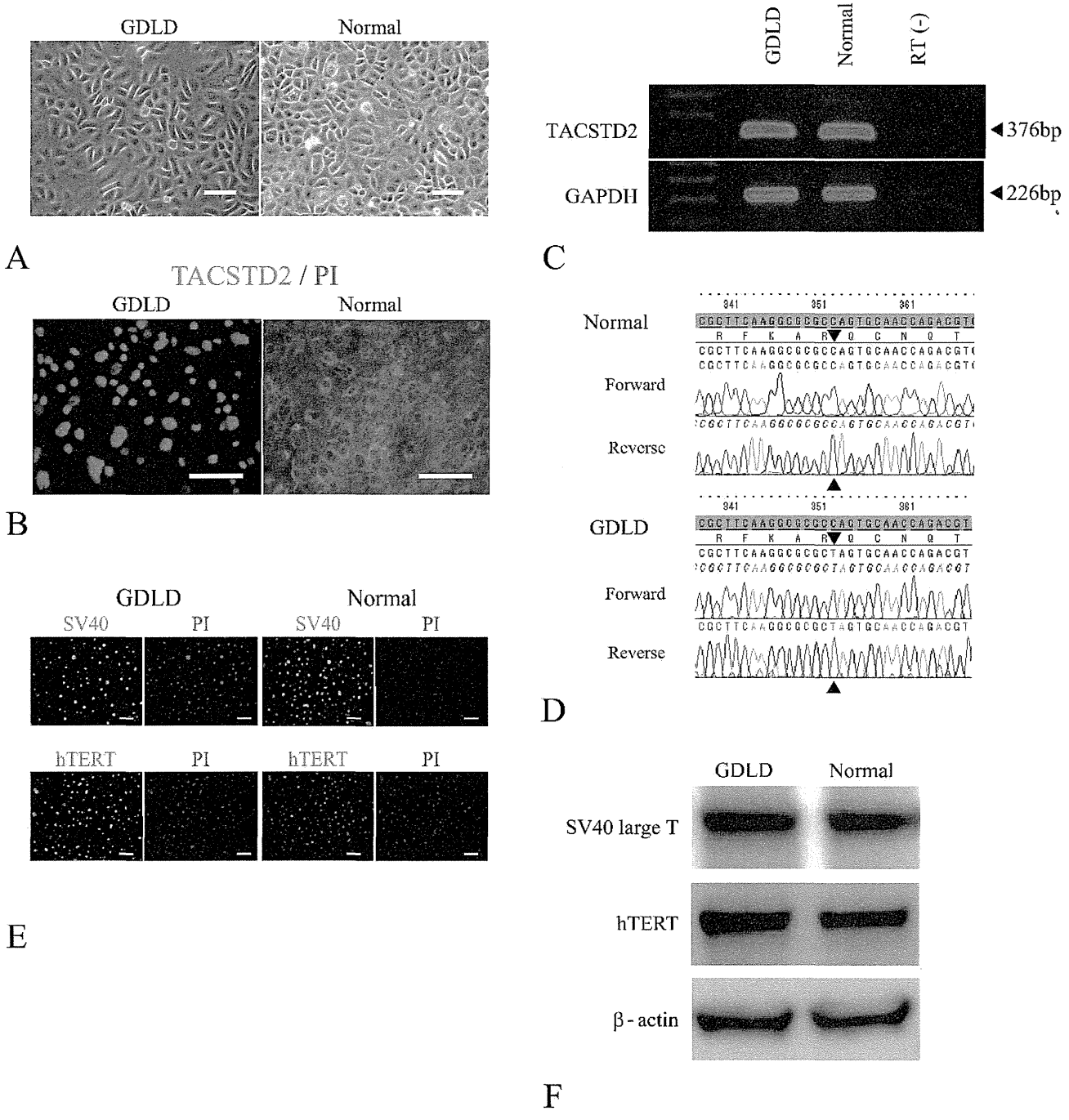

Figure 2. Characteristics of the imHCE_GDLD cells and of the imHCE_normal cells. **(A)** Both cell lines exhibited similar cell size and cell shape, demonstrating an organized cobblestone appearance by phase contrast microscopy. **(B)** The imHCE_GDLD cells were devoid of the TACSTD2 protein, but the imHCE_normal cells expressed the protein. **(C)** At the RNA level, both cell lines expressed the TACSTD2 gene almost at the same level. GAPDH was investigated as an internal control. **(D)** Sequencing analysis detected the p.Gln118X mutation in the RT-PCR product of the imHCE_GDLD cells. Both cell lines expressed the SV40 large T antigen and hTERT proteins, as judged by immunostaining **(E)** as well as Western blot **(F)** analyses. *Scale bars* in the immunostaining analysis correspond to 100 μm. The immortalized corneal epithelial cell line from the GDLD patient and the immortalized corneal epithelial cell line forming the normal cornea are abbreviated respectively as imHCE_GDLD and imHCE_normal.

almost identical level and with an almost identical immunolocalization pattern (Fig. 4C). Confocal microscopy analysis revealed that the immunolocalization of the CLDN1 and CLDN7 proteins exhibited a pattern with dots, many of which seemed to exist on the plasma membrane in the imHCE_GDLD cells, although it exhibited the membrane-bound pattern in the imHCE_normal cells (Fig. 4D).

Preliminary Study of Gene Therapy for the Treatment of GDLD Corneas

Finally, we conducted a preliminary study to investigate whether gene therapy is beneficial for the treatment of GDLD corneas. We expected that exogenous introduction of the wild type TACSTD2 gene might normalize the disease situation

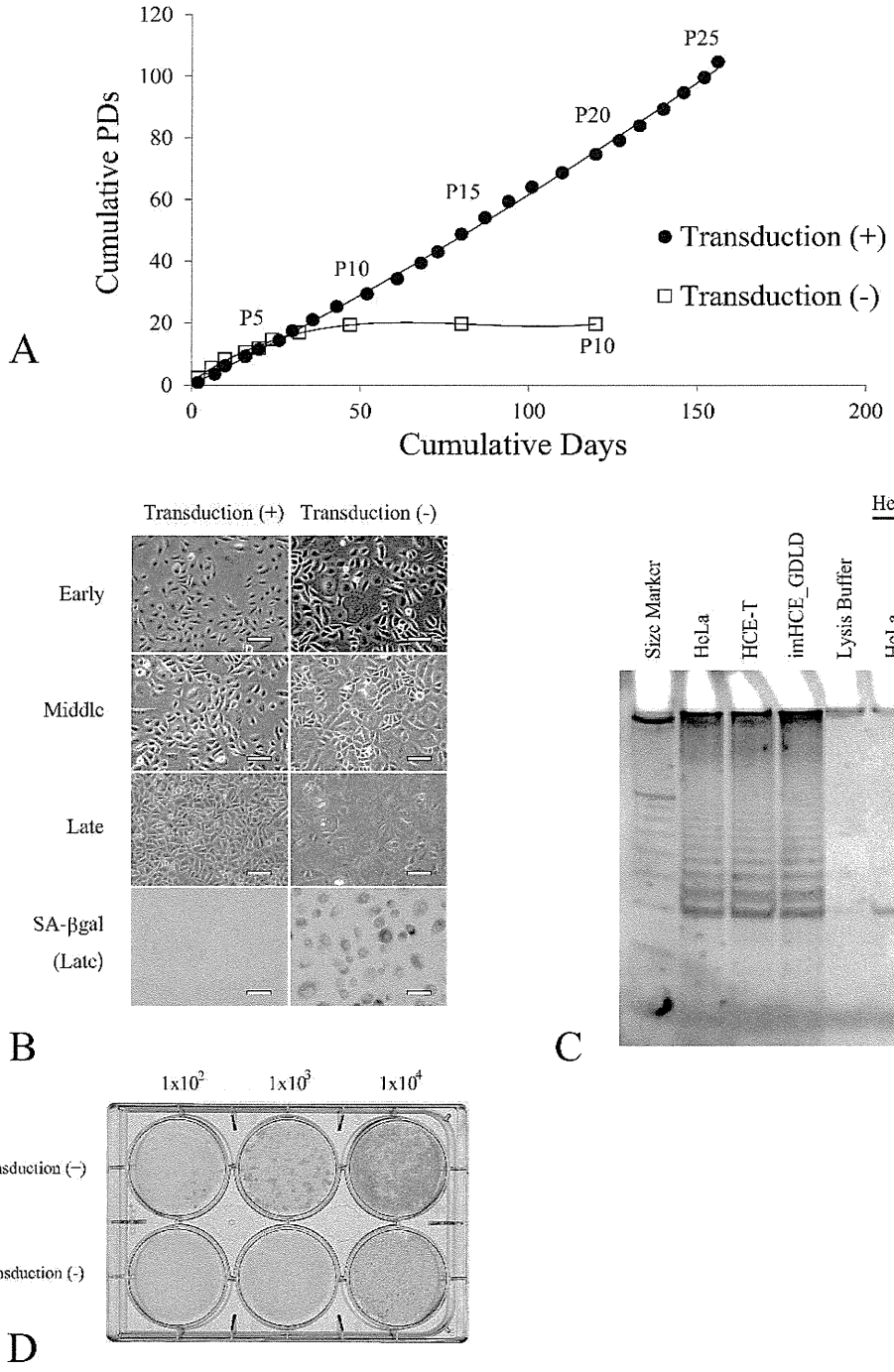

Figure 3. Cell growth kinetics, senescence status, telomerase activity, and colony-forming activity of the immortalized corneal epithelial cells of the GDLD patient. (**A**) PD analysis revealed that the GDLD corneal epithelial cells continued to proliferate with the transduction of the two genes (SV40 large T antigen and hTERT genes), whereas the nontransduced cells stopped proliferating at their early stage of culture. (*P numbers* represent the number of passages, not the PD number.) (**B**) The morphology and the senescence status were assessed in the transduced cells or in nontransduced cells at the early (3.5 PDs and 3.2 PDs, respectively), middle (11.5 PDs and 11.8 PDs, respectively), and late (54.1 PDs and 19.4 PDs, respectively) stages of culture. The transduced cells maintained their small and square cell morphology, although the nontransduced cells gradually exhibited large and flattened cell morphology. The senescence status was assessed using SA-βgal assay in both transduction (+) and (−) cells at their late (54.1 PDs and 19.4 PDs, respectively) stages of culture. Most of the nontransduced cells exhibited apparent *blue staining* in their cytoplasmic area, whereas the transduced cells did not. *Scale bars*: 100 μm. (**C**) Telomerase activity was assessed using TRAP assay for HeLa cells (*lanes 2* and *6*), immortalized human corneal epithelial cells (HCE-T, *lanes 3* and *7*), and the immortalized GDLD corneal epithelial cells (imHCE_GDLD, *lanes 4* and *8*). For the negative controls, lysis buffer (*lane 5*) and heat-inactivated lysates of the above cell types (*lanes 6–8*) were investigated. *Lane 1* shows the size marker. The HeLa cells, the HCE-T cells, and the immortalized GDLD corneal epithelial cells exhibited clear laddering of TRAP products, indicating the telomerase activity in these cells. (**D**) Colony-forming assay was performed for the transduced or nontransduced corneal epithelial cells from the GDLD patient. The transduced cells produced multiple-cell expansion foci that were significantly larger and more numerous than the nontransduced cells.

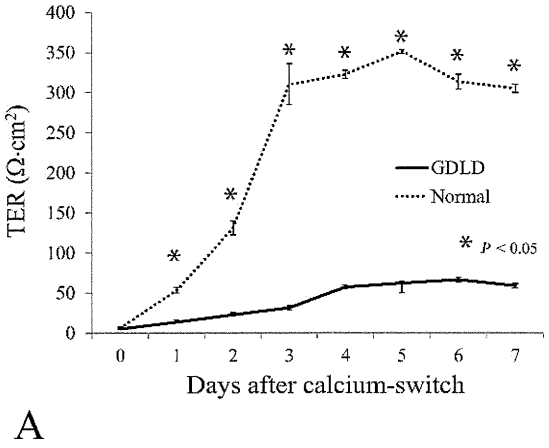

A

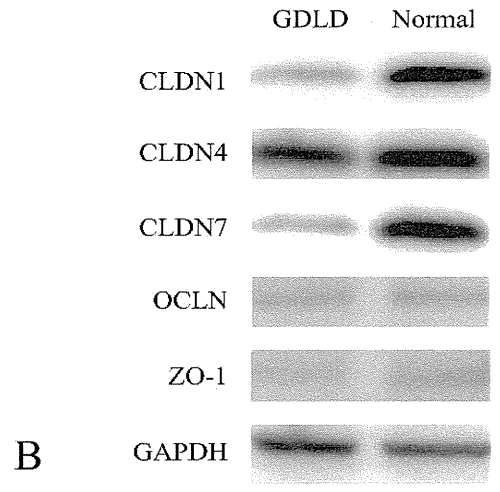

B

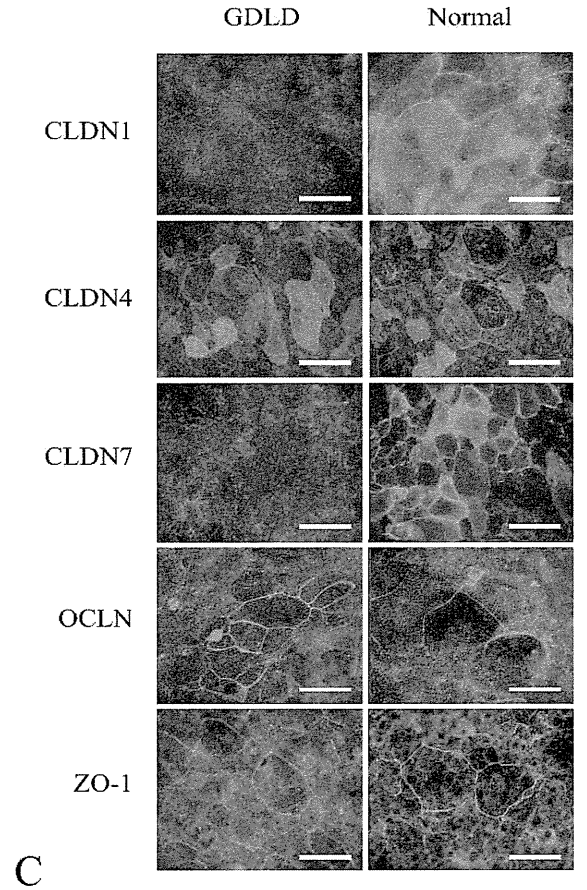

C

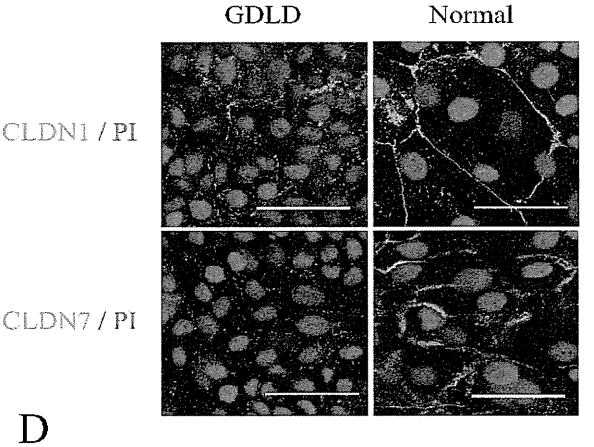

D

FIGURE 4. Epithelial barrier function and the expression of tight-junction-related proteins were investigated in imHCE_GDLD. (**A**) The epithelial barrier function was investigated by measuring the trans-epithelial resistance (TER). The TER of the imHCE_GDLD cells was significantly lower than that of the imHCE_normal. The experiments were done in triplicate, with data presented as mean ± SD. $^*P < 0.05$ (Student's *t*-test). Expression of the tight-junction-related proteins including CLDN 1, 4, and 7; OCLN; and ZO-1 were analyzed using Western blot (**B**) and immunostaining (**C**) analyses in the imHCE_GDLD and imHCE_normal cells. (**B**) The expression levels of the CLDN1 and CLDN7 proteins were significantly lower in the imHCE_GDLD cells than in the imHCE_normal cells. (**C**) The immunostaining patterns of the CLDN1 and CLDN7 proteins in the imHCE_GDLD cells differed dramatically from those in the imHCE_normal cells. The other three tight-junction-related proteins exhibited an almost identical immunostaining pattern and an almost identical expression level in both the imHCE_GDLD and imHCE_normal cells. GAPDH was investigated as a loading control in Western blotting. *Scale bars*: 100 μm. (**D**) Subcellular localization of the CLDN1 and CLDN7 proteins was investigated further using confocal microscopy. The immunolocalization patterns of the CLDN1 and CLDN7 proteins were dot-like with many dots presumably lining the plasma membrane in the imHCE_GDLD cells, but with a membrane-bound pattern in the imHCE_normal cells. *Scale bars*: 50 μm. The immortalized corneal epithelial cell line from the GDLD patient and the immortalized corneal epithelial cell line from the normal cornea are abbreviated as imHCE_GDLD and imHCE_normal, respectively.

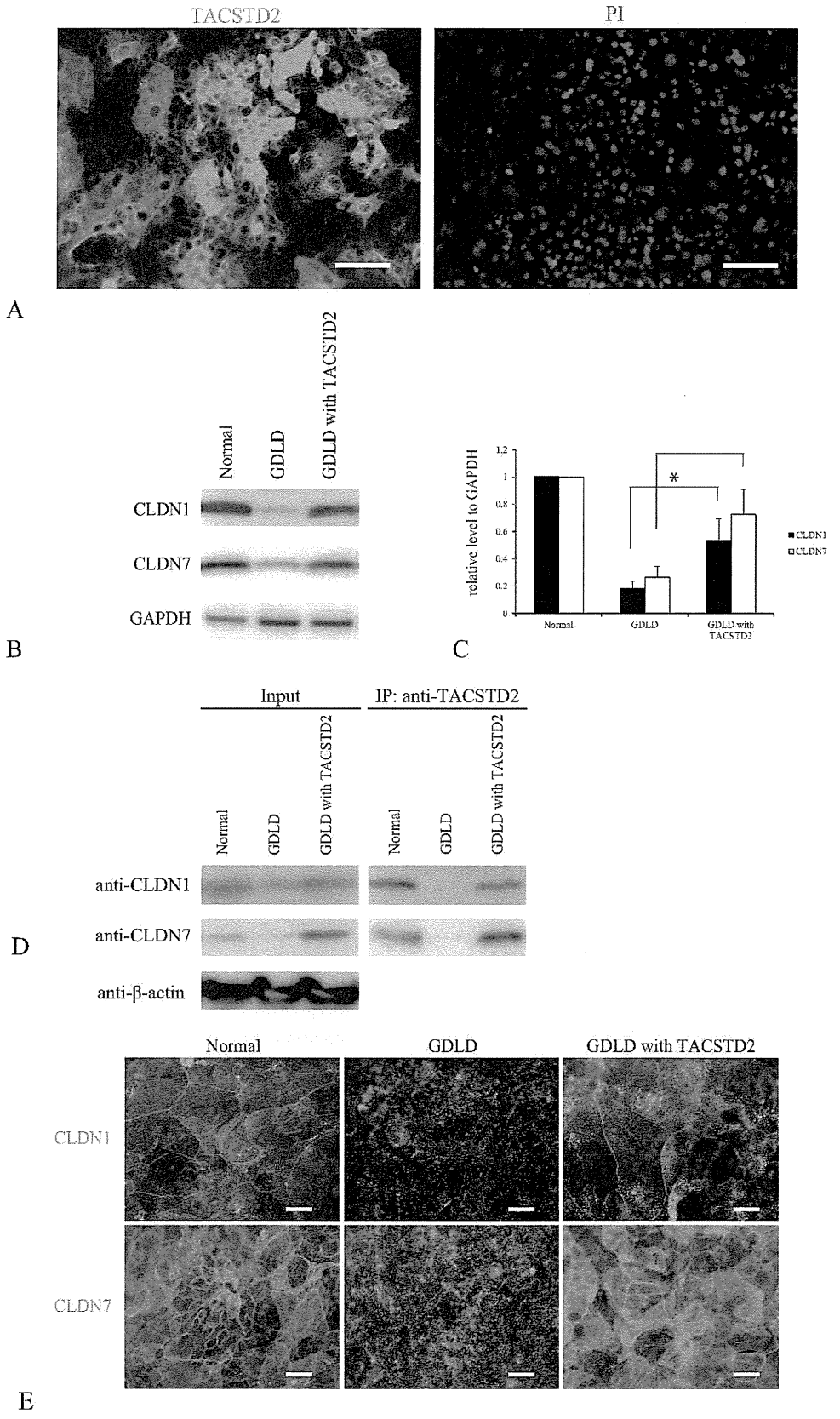

FIGURE 5. Preliminary study of gene therapy for GDLD cornea. The imHCE_GDLD was transduced with a lentiviral vector expressing the wild-type TACSTD2 protein. (**A**) Approximately 70% of the imHCE_GDLD cells were positive for the TACSTD2 protein. Transduction efficiency was estimated by counting the TACSTD2 positive cells from randomly selected immunostaining images. *Scale bars*: 100 μm. (**B**) Western blot analysis demonstrates the remarkable upregulation of the CLDN1 and CLDN7 proteins after the transduction of the wild-type TACSTD2 gene in the imHCE_GDLD cells. (**C**) Results of Western blot analyses were quantitated using densitometry. The bar graph shows the relative level of the CLDN1 and CLDN7 proteins to the GAPDH protein. $^*P < 0.05$ (Student's *t*-test). (**D**) Immunoprecipitation assay revealed that the TACSTD2 protein binds to the CLDN1 and CLDN7 proteins. (**E**) Results of the immunostaining analysis against the imHCE_normal, the imHCE_GDLD, and

the TACSTD2 gene transduced imHCE_GDLD cells. The transduction of the wild-type TACSTD2 gene almost completely normalized the subcellular localization of the CLDN1 and CLDN7 proteins in the imHCE_GDLD. *Scale bars*: 50 μm. The immortalized corneal epithelial cell line from the GDLD patient and the immortalized corneal epithelial cell line from the normal cornea are abbreviated as imHCE_GDLD and imHCE_normal, respectively.

occurring in GDLD cornea because GDLD is a monogenic disorder caused by the biallelic loss of function mutation of the TACSTD2 gene. The imHCE_GDLD cells were transduced with the wild-type TACSTD2 gene by the lentivirus, with transduction efficiency as high as approximately 70% (Fig. 5A). The exogenous transduction of the wild-type TACSTD2 gene significantly increased the expression levels of the CLDN1 and CLDN7 proteins (Figs. 5B, 5C). The exogenously transduced wild-type TACSTD2 protein was found to be bound to the CLDN1 and CLDN7 proteins, as judged by immunoprecipitation analysis (Fig. 5D). In addition, the exogenous transduction of the wild-type TACSTD2 gene almost completely normalized the subcellular localization of the CLDN1 and CLDN7 proteins (Fig. 5E).

Discussion

In this study, we established the immortalized corneal epithelial cells from a GDLD patient by the transfection of SV40 large T antigen and hTERT genes. The cell line has high proliferation activity after their cumulative PDs exceed 100 and exhibits significant reduction of the barrier function, which is the major characteristic of corneal epithelial cells in a GDLD patient. Furthermore, the cell line exhibited decreased expression of the CLDN1 and CLDN7 proteins as well as the altered subcellular localization of these proteins, which shows good agreement with the in vivo GDLD cornea. Therefore, the established cell line, which well reflects the disease situation of the GDLD cornea, might be a good in vitro model for a GDLD cornea.

Normal human cells usually stop dividing at approximately 40 to 60 PDs, depending on several factors such as the age of their origin, the cell type, and the culture condition.[30] In general, the expansion of the life-span of a cell encounters a two-step barrier: senescence (M1) and crisis (M2).[31] The two replicative barriers have been shown to play a crucial role mainly in limiting the progress of tumorigenesis,[32] which is a life-threatening situation in most multicellular organisms. The M1 replicative barrier is known to be operated by two crucial tumor-suppressor genes: the retinoblastoma (RB) gene and the p53 gene. The nuclear Rb protein binding prevents accessibility of the transcription factor E2F to nuclear cyclins (E and A). Upon stimulation by growth factor receptor signals, the Rb protein is phosphorylated. It releases E2F, which can enable the activation of these S phase-related cyclins.[33] The M2 replicative barrier is known to be achieved by the shortening of telomeres, which might be attributable to the silencing of the hTERT gene expression in stem cells and others in the human body, with the notable exception being expression in germline cells.[24] Some virus-derived proteins such as the SV40 large T antigen and human papilloma virus E6/E7 proteins are known to bind to the RB and p53 proteins to abrogate their tumor-suppressive activity, resulting in the bypass of cells from the M1 stage.[34,35] The hTERT gene is known to be the rate-limiting factor in the telomerase activity, whereas other components of the telomerase-holoenzyme complex are known to be expressed constitutively in cells of many types.[36] Reportedly, the forced expression of only the hTERT gene was sufficient for the acquisition of telomerase activity.[37]

Several reports have described the immortalization of cells by single-gene transduction with SV40 large T antigen[29,35] or hTERT gene.[37,38] However, because each of the two replicative barriers M1 and M2 has strong inhibitive power to suppress cell expansion, it might be generally accepted that single-gene transduction with either of the two genes has markedly lower potential to achieve immortalization than that with both genes. It can be speculated that the reported immortalization by the single-gene transduction with either of the two genes might be at least partially attributable to the spontaneous repression of either or both RB and p53 gene(s), or the spontaneous activation of the endogenous hTERT gene, possibly because of gene mutation[39] or epigenetic alteration.[40] Since the starting cell number of our GDLD corneal epithelial cells was limited, we theorized that the immortalization process might fail if its efficiency was not high. Therefore, we chose to use both genes to easily overcome the M1 and M2 replicative barriers.

As for the development of a new therapy, the transduction of the wild-type TACSTD2 gene to the patient's corneal epithelial cells can be a promising therapy because GDLD is a monogenic disorder caused by the biallelic loss of function mutation of the TACSTD2 gene. Therefore, the transduction of the wild-type TACSTD2 gene might normalize the disease situation in the GDLD corneal epithelial cells. However, before the clinical application of the gene therapy, several issues must be resolved. Physicians must ascertain the optimal dosage of the transduced gene because, in general, faint expression would have little therapeutic effect, although overexpression might engender unanticipated side effects. For the TACSTD2 gene, overexpression of the gene might present a risk for tumorigenesis because the gene is presumably oncogenic.[41] We performed a preliminary experiment as for the gene therapy of GDLD. Approximately 70% imHCE_GDLD cells were transduced with the wild-type TACSTD2 gene. The gene transduction normalized the disease situation of corneal epithelial cells of GDLD, with increased expression of the CLDN1 and 7 proteins and altered subcellular localization of the two proteins from cytoplasm to plasma membrane. Unfortunately, after multiple repetitions of experiments, which yielded all of these promising data, we were unable to obtain the normalization of TER, perhaps because of the insufficiency of the transduction efficiency. Direct gene correction by artificial nucleases such as zinc finger nuclease and TAL effector nuclease presents another avenue for gene therapy.

In summary, the results of this study demonstrate the establishment of an immortalized corneal epithelial cell line from this GDLD patient. Currently, we are only halfway along in our understanding of GDLD pathophysiology. Moreover, no single prominent advance has occurred during the last decade in the development of novel effective treatments for GDLD. We hope that this newly established cell line will help foster breakthroughs in the examination of these important issues.

Acknowledgments

The authors thank John Bush for his excellent help in the preparation of the manuscript. We also thank the staff members at the Northwest Lions Eye Bank Foundation for helping us obtain the fresh human cornea used for this study.

Supported by Grant-in-Aid 21592238 from the Japanese Ministry of Education, Culture, Sports, Science and Technology and Grant H23-Nanchi-Ippan-084 from the Japanese Ministry of Health, Labour and Welfare. This work was also supported by research funds from the Kyoto Foundation for the Promotion of Medical Science. The authors alone are responsible for the content and writing of the paper.

Disclosure: **K. Kitazawa**, None; **S. Kawasaki**, None; **K. Shinomiya**, None; **K. Aoi**, None; **A. Matsuda**, None; **T. Funaki**, None; **K. Yamasaki**, None; **M. Nakatsukasa**, None; **N. Ebihara**, None; **A. Murakami**, None; **J. Hamuro**, None; **S. Kinoshita**, None

References

1. Nakaizumi G. A rare case of corneal dystrophy. *Acta Soc Ophthalmol Jpn.* 1914;18:949-950.
2. Gartry DS, Falcon MG, Cox RW. Primary gelatinous drop-like keratopathy. *Br J Ophthalmol.* 1989;73:661-664.
3. Mondino BJ, Rabb MF, Sugar J, Sundar Raj CV, Brown SI. Primary familial amyloidosis of the cornea. *Am J Ophthalmol.* 1981;925:732-736.
4. Weber FL, Babel J. Gelatinous drop-like dystrophy: a form of primary corneal amyloidosis. *Arch Ophthalmol.* 1980;98:144-148.
5. Fukjiki K, Kanai A, Nakajima A. Gelatinous drop-like corneal dystrophy in Japanese population [abstract]. In: Vogel F, Sperling K, eds. *Proceedings of the 7th International Congress of Human Genetics.* Berlin, Germany: Springer-Verlag; 1986;248-249.
6. Kawano H, Fujiki K, Kanai A. Prevalence of gelatinous drop-like corneal dystrophy in Japan [in Japanese]. *Atarashii Ganka.* 1992;9:1879-1882.
7. Tsujikawa M, Kurahashi H, Tanaka T, et al. Identification of the gene responsible for gelatinous drop-like corneal dystrophy. *Nat Genet.* 1999;21:420-423.
8. Tsujikawa M, Kurahashi H, Tanaka T, et al. Homozygosity mapping of a gene responsible for gelatinous drop-like corneal dystrophy to chromosome 1p. *Am J Hum Genet.* 1998;63:1073-1077.
9. Cortina MS, Porter IW, Sugar J, de la Cruz J. Boston type I keratoprosthesis for visual rehabilitation in a patient with gelatinous drop-like corneal dystrophy. *Cornea.* 2012;31:844-845.
10. Ito M, Takahashi J, Sakimoto N. Histological study of gelatinous drop-like dystrophy following excimer laser phototherapeutic keratectomy [in Japanese]. *Nippon Ganka Gakkai Zasshi.* 2000;104:44-50.
11. Uhlig CE, Groppe M, Busse H, Saeger W. Morphological and histopathological changes in gelatinous drop-like corneal dystrophy during a 15-year follow-up. *Acta Ophthalmol.* 2010;88:e273-e274. Available at: http://onlinelibrary.wiley.com/doi/10.1111/j.1755-3768.2009.01708.x/pdf. Accessed August 8, 2013.
12. Nagataki S, Tanishima T, Sakimoto T. A case of primary gelatinous drop-like corneal dystrophy. *Jpn J Ophthalmol.* 1972;16:107-116.
13. Ohzono S, Ogawa K, Kinoshita S, Moriyama H, Manabe R. Recurrence of corneal dystrophy following keratoplasty [in Japanese]. *Rinsho Ganka.* 1984;38:747-749.
14. Shinozaki K, Yoshino K, Yamagami H, Takamura E. Histochemical examination of recurrent cornea gelatinous drop-like dystrophy [abstract]. *Invest Ophthalmol Vis Sci Suppl.* 1996;37:S1020.
15. Wang J, Zhang K, Grabowska D, et al. Loss of Trop2 promotes carcinogenesis and features of epithelial to mesenchymal transition in squamous cell carcinoma. *Mol Cancer Res.* 2011;9:1686-1695.
16. Alberti S, Miotti S, Stella M, et al. Biochemical characterization of Trop-2, a cell surface molecule expressed by human carcinomas: formal proof that the monoclonal antibodies T16 and MOv-16 recognize Trop-2. *Hybridoma.* 1992;11:539-545.
17. Ripani E, Sacchetti A, Corda D, Alberti S. Human Trop-2 is a tumor-associated calcium signal transducer. *Int J Cancer.* 1998;76:671-676.
18. Nakatsukasa M, Kawasaki S, Yamasaki K, et al. Tumor-associated calcium signal transducer 2 is required for the proper subcellular localization of claudin 1 and 7: implications in the pathogenesis of gelatinous drop-like corneal dystrophy. *Am J Pathol.* 2010;177:1344-1355.
19. Fradet Y, Cordon-Cardo C, Thomson T, et al. Cell surface antigens of human bladder cancer defined by mouse monoclonal antibodies. *Proc Natl Acad Sci U S A.* 1984;81:224-228.
20. Weiss JS, Moller HU, Lisch W, et al. The IC3D classification of the corneal dystrophies. *Cornea.* 2008;27(suppl 2):S1-S83.
21. Kawasaki S, Kinoshita S. Clinical and basic aspects of gelatinous drop-like corneal dystrophy. *Dev Ophthalmol.* 2011;48:97-115.
22. Yamasaki K, Kawasaki S, Young RD, et al. Genomic aberrations and cellular heterogeneity in SV40-immortalized human corneal epithelial cells. *Invest Ophthalmol Vis Sci.* 2009;50:604-613.
23. Majo F, Rochat A, Nicolas M, Jaoude GA, Barrandon Y. Oligopotent stem cells are distributed throughout the mammalian ocular surface. *Nature.* 2008;456:250-254.
24. Kim NW, Piatyszek MA, Prowse KR, et al. Specific association of human telomerase activity with immortal cells and cancer. *Science.* 1994;266:2011-2015.
25. Mitchell JR, Wood E, Collins K. A telomerase component is defective in the human disease dyskeratosis congenita. *Nature.* 1999;402:551-555.
26. Nakayama J, Saito M, Nakamura H, Matsuura A, Ishikawa F. TLP1: a gene encoding a protein component of mammalian telomerase is a novel member of WD repeats family. *Cell.* 1997;886:875-884.
27. Feng J, Funk WD, Wang SS, et al. The RNA component of human telomerase. *Science.* 1995;269:1236-1241.
28. Scherer WF, Syverton JT, Gey GO. Studies on the propagation in vitro of poliomyelitis viruses. IV. Viral multiplication in a stable strain of human malignant epithelial cells (strain HeLa) derived from an epidermoid carcinoma of the cervix. *J Exp Med.* 1953;97:695-710.
29. Araki-Sasaki K, Ohashi Y, Sasabe T, et al. An SV40-immortalized human corneal epithelial cell line and its characterization. *Invest Ophthalmol Vis Sci.* 1995;36:614-621.
30. Hayflick L. The limited in vitro lifetime of human diploid cell strains. *Exp Cell Res.* 1965;37:614-636.
31. Wright WE, Pereira-Smith OM, Shay JW. Reversible cellular senescence: implications for immortalization of normal human diploid fibroblasts. *Mol Cell Biol.* 1989;9:3088-3092.
32. Shay JW, Wright WE, Werbin H. Defining the molecular mechanisms of human cell immortalization. *Biochim Biophys Acta.* 1991;1072:1-7.
33. Shirodkar S, Ewen M, DeCaprio JA, et al. The transcription factor E2F interacts with the retinoblastoma product and a p107-cyclin A complex in a cell cycle-regulated manner. *Cell.* 1992;68:157-166.
34. Bryan TM, Reddel RR. SV40-induced immortalization of human cells. *Crit Rev Oncog.* 1994;5:331-357.
35. Wilson SE, Weng J, Blair S, He YG, Lloyd S. Expression of E6/E7 or SV40 large T antigen-coding oncogenes in human corneal endothelial cells indicates regulated high-proliferative capacity. *Invest Ophthalmol Vis Sci.* 1995;36:32-40.
36. Weinrich SL, Pruzan R, Ma L, et al. Reconstitution of human telomerase with the template RNA component hTR and the catalytic protein subunit hTRT. *Nat Genet.* 1997;17:498-502.

37. Bodnar AG, Ouellette M, Frolkis M, et al. Extension of life-span by introduction of telomerase into normal human cells. *Science*. 1998;279:349-352.
38. Offord EA, Sharif NA, Mace K, et al. Immortalized human corneal epithelial cells for ocular toxicity and inflammation studies. *Invest Ophthalmol Vis Sci*. 1999;40:1091-1101.
39. Guimaraes DP, Hainaut P. TP53: a key gene in human cancer. *Biochimie*. 2002;84:83-93.
40. Renaud S, Loukinov D, Abdullaev Z, et al. Dual role of DNA methylation inside and outside of CTCF-binding regions in the transcriptional regulation of the telomerase hTERT gene. *Nucleic Acids Res*. 2007;35:1245-1256.
41. Wang J, Day R, Dong Y, Weintraub SJ, Michel L. Identification of Trop-2 as an oncogene and an attractive therapeutic target in colon cancers. *Mol Cancer Ther*. 2008;7:280-285.

Investigative Ophthalmology & Visual Science

STEM CELLS®
TISSUE-SPECIFIC STEM CELLS

Corneal Endothelial Cell Fate Is Maintained by LGR5 Through the Regulation of Hedgehog and Wnt Pathway

KANA HIRATA-TOMINAGA,[a] TAKAHIRO NAKAMURA,[a,b] NAOKI OKUMURA,[a,c] SATOSHI KAWASAKI,[a] EUNDUCK P. KAY,[c] YANN BARRANDON,[d] NORIKO KOIZUMI,[a,c] SHIGERU KINOSHITA[a]

[a]Department of Ophthalmology, Kyoto Prefectural University of Medicine, Kyoto, Japan; [b]Research Center for Inflammation and Regenerative Medicine, Doshisha University, Kyoto, Japan; [c]Department of Biomedical Engineering, Faculty of Life and Medical Sciences, Doshisha University, Kyotanabe, Japan; [d]Laboratory of Stem Cell Dynamics, Ecole Polytechnique Federale de Lausanne, Lausanne, Switzerland

Key Words. Cornea • Endothelium • Stem cell • LGR5 • Hedgehog • Wnt

ABSTRACT

Leucine-rich repeat-containing G protein-coupled receptor 5 (LGR5), a target of Wnt signaling, is reportedly a marker of intestine, stomach, and hair follicle stem cells in mice. To gain a novel insight into the role of LGR5 in human corneal tissue, we performed gain- and loss-of-function studies. The findings of this study show for the first time that LGR5 is uniquely expressed in the peripheral region of human corneal endothelial cells (CECs) and that LGR5$^{(+)}$ cells have some stem/progenitor cell characteristics, and that in human corneal endothelium, LGR5 is the target molecule and negative feedback regulator of the Hedgehog (HH) signaling pathway. Interestingly, the findings of this study show that persistent LGR5 expression maintained endothelial cell phenotypes and inhibited mesenchymal transformation (MT) through the Wnt pathway. Moreover, R-spondin-1, an LGR5 ligand, dramatically accelerated CEC proliferation and also inhibited MT through the Wnt pathway. These findings provide new insights into the underlying homeostatic regulation of human corneal endothelial stem/progenitor cells by LGR5 through the HH and Wnt pathways. STEM CELLS *2013;31:1396–1407*

Disclosure of potential conflicts of interest is found at the end of this article.

INTRODUCTION

In most vertebrates, including humans and other primates, the majority of external information is gained through eyesight, and the cornea is a very important avascular tissue related to the maintenance of this vision system. The cornea consists of a stratified surface epithelial cell layer, a thick collagenous stroma, and an inner single-cell-layered endothelium. Through the combination of these three cell layers, corneal tissue is kept optically clear, and ocular homeostasis and integrity are maintained. According to the World Health Organization, an estimated 25-million people worldwide are affected by cornea-related blindness [1]. Therefore, it is important to understand the underlying mechanisms by which corneal integrity is maintained.

From the medical standpoint, corneal endothelial cells (CECs) represent the most important component of the cornea, as they are crucial for maintaining corneal integrity [2]. CECs, which are derived from the neural crest, play an essential role in the maintenance of corneal transparency through their barrier and pump functions. Although human CECs are mitotically inactive and are arrested at the G1 phase of the cell cycle in vivo [3], they retain the capacity to proliferate in vitro [4]. However, a recent study has shown that to date, culturing human CECs for a long period of time is extremely difficult [5]. In view of these findings, it is now understood that the molecular mechanism, including the stem cell biology of corneal endothelial behavior, is an important research subject to explore to better understand the role and function of the cornea, as well as to elucidate the most effective means by which to reconstruct damaged corneal tissue.

It is well known that stem cells facilitate the maintenance of self-renewing tissues and organs [6–8]. With regard to corneal tissue, various studies indicate that corneal epithelial stem cells reside in the basal layer of the peripheral cornea in the limbal zone [9–11]. In contrast, even though it has been reported that CECs from the peripheral area of the cornea retain higher replication ability [12], the corneal endothelial stem cells have yet to be specifically identified and their exact locations are also not fully understood owing to the lack of unique markers and the absence of stem cell assay [13–15].

Recently, genetic mouse models have allowed for the visualization, isolation, and genetic marking of leucine-rich

Author contributions: K.H.-T.: provision of study material or patients, collection and/or assembly of data; T.N.: conception and design, collection and/or assembly of data, data analysis and interpretation, writing manuscript; N.O.: collection and/or assembly of data, S. KAWASAKI: collection and/or assembly of data; E.P.K.: data analysis and interpretation; Y.B.: financial support; N.K.: data analysis and interpretation; financial support; S. KINOSHITA: collection and/or assembly of data. K.H.T. and T.N. contributed equally to this article.

Correspondence: Takahiro Nakamura, M.D., Ph.D., Department of Ophthalmology, Kyoto Prefectural University of Medicine, 465 Kajii-cho, Hirokoji-agaru, Kawaramachi-dori, Kamigyo-ku, Kyoto 602-0841, Japan. Telephone: +81-75-251-5578; Fax: +81-75-251-5663; e-mail: tnakamur@koto.kpu-m.ac.jp Received September 18, 2012; accepted for publication March 4, 2013; first published online in STEM CELLS *EXPRESS* April 3, 2013. 1066-5099/2013/$30.00/0 doi: 10.1002/stem.1390

repeat G protein-coupled receptor 5 (LGR5)-positive cells and have provided evidence that there are stem cells in the stomach, small intestine, colon, and hair follicles of those mice [16–18]. LGR5 reportedly is expressed downstream of Hedgehog (HH) signaling in basal cell carcinoma, and $LGR5^{high}$ cells in hair follicles reportedly show active HH signaling [16, 19]. To gain more insights on the mechanism of corneal stem cells, we performed Affymetrix Microarray (Affymetrix, Inc., Santa Clara, CA) analyses using holoclone-type human corneal keratinocytes, and LGR5 was identified as a potential marker for human corneal keratinocyte stem/progenitor cells (data not shown). These findings have led us to an interesting hypothesis that a common stem cell marker exists between developmentally distinct tissues, yet to date, there have been no reports regarding the role and function of LGR5 in CECs.

In this study, we show for the first time that LGR5 is uniquely expressed in the peripheral region of human CECs and that $LGR5^+$ cells have some stem/progenitor cell characteristics. In addition, the findings of this study show that LGR5 is a key molecule for maintaining the integrity of CECs and is mainly regulated by HH and Wnt signaling. Moreover, R-spondin-1 (RSPO1), an LGR5 ligand, was found to dramatically influence the maintenance of CECs. Thus, our data provide new insights into the underlying homeostatic regulation of corneal endothelial stem/progenitor cells by LGR5.

Materials and Methods

Tissues

All human donor cornea tissues were obtained from SightLife (Seattle, WA) eye bank, and all corneas were stored at 4°C in storage medium (Optisol; Bausch&Lomb, Rochester, NY, http://www.bausch.com). A total of 80 donor corneas were used for all experiments (donor age: 61.8 ± 8.6 years (mean ± SD); mean time to preservation: 7.6 ± 5.6 hours; mean endothelial cell density: $2{,}757 \pm 221$ mm^2; mean storage time: 6.0 ± 0.9 days). All experiments were performed in accordance with the tenets set forth in the Declaration of Helsinki. Eight corneas obtained from cynomolgus monkeys (donor age: 7.1 ± 4.5 years (mean ± SD); estimated equivalent human age: 15–42 years) housed at NISSEI BILIS Co., Ltd., Koka, Japan and Eve Bioscience, Co., Ltd., Japan, respectively, were used for this study. For other research purposes, the monkeys were given an overdose of sodium pentobarbital for euthanization intravenously according to the approval by the Laboratory Animal Use and Ethics Committee of the Shiga Laboratory, NISSEI BILIS Co., Ltd. and the institutional animal care and use committee of Eve Bioscience, Co., Ltd., respectively. The corneas of the cynomolgus monkeys were harvested after confirmation of cardiopulmonary arrest by veterinarians, and were then provided for our research. All corneas were stored at 4°C in Optisol storage medium for less than 24 hours before the experiment. All animals were housed and treated in accordance with the The Association for Research in Vision and Ophthalmology Statement for the Use of Animals in Ophthalmic and Vision Research.

Antibodies and Reagents

For immunohistochemistry and flow cytometry, the following rabbit polyclonal antibodies were used: anti-C-terminal domain of human LGR5 (71143; GeneTex Inc., San Antonio, TX) and anti-ZO1 (40-2200; Zymed Laboratories Inc., South San Francisco, CA, http://www.invitrogen.com/content.cfm?pageid11356). The following mouse monoclonal antibodies were used: anti-Na^+/K^+ ATPase (05-369; EMD Millipore Corporation, Billerica, MA http://www.emdmillipore.com), anti-Ki67, and anti-β-catenin (556003, 610153; BD Biosciences, Franklin Lakes, NJ http://www.bdbiosciences.com/home.jsp). Secondary antibodies were Alexa Fluor-488 goat anti-rabbit or mouse IgG (A11034, A11029; Molecular Probes Inc., Eugene, OR, http://www.invitrogen.com/site/us/en/home/brands/Molecular-Probes.html) and Cy3 anti-mouse IgG (715-165-150; Jackson Immunoresearch Laboratories, Inc., West Grove, PA, http://www.jacksonimmuno.com). For Western blotting, the following rabbit polyclonal antibodies were used: anti-LRP6 and p-LRP6 (3395, 2568; Cell Signaling Technology, Inc., Beverly, MA, http://www.cellsignal.com). The following mouse monoclonal antibodies were used: β-catenin (BD Biosciences) and β-actin (A5441; Sigma-Aldrich, St. Louis, MO, http://www.sigmaaldrich.com). Secondary antibodies were horse radish peroxide (HRP)-conjugated anti-rabbit or mouse IgG (NA934, NA931; GE Healthcare, Piscataway, NJ, http://www.gehealthcare.com). Recombinant human sonic HH (SHH), purmorphamine, cyclopamine, and RSPOs were purchased from R&D Systems Inc. (Minneapolis, MN, http://www.rndsystems.com).

Cell Culture

The human and monkey CECs were cultured using the method of our previously reported system [2, 20–22]. Briefly, the Descemet's membrane including CECs was stripped and digested with 2 mg/ml collagenase A (Roche Applied Science, Penzberg, Germany, http://www.roche-applied-science.com) at 37°C. After incubation for 3 hours, the CECs (individual cells and cell aggregates) obtained from individual corneas were resuspended in culture medium containing Opti-MEM-I (Invitrogen), 5% fetal bovine serum (FBS), 50 μg/ml gentamicin, and 10 μM Y-27632 (Calbiochem, LA Jolla, CA) and then plated in one well of a 12-well plate coated with FNC Coating Mix (Athena Environmental Sciences, Inc., Baltimore, MD, http://www.athenaes.com). The CECs were cultured in a humidified atmosphere at 37°C in 5% CO_2. The culture medium was changed every 2 days. When cells reached subconfluence, they were rinsed in Ca^{2+} and Mg^{2+}-free phosphate-buffered saline (PBS), trypsinized with TrypLE Select (Life Technologies) for 10 minutes at 37°C, and passaged at ratios of 1:2–4.

Immunohistochemistry

Immunohistochemical studies followed our previously described method [23, 24]. Briefly, 8-μm-thin sections and whole-mount sections prepared by peeling the Descemet's membrane from cornea tissues were placed on silane-coated slides, air dried, and fixed in 100% acetone at 4°C for 15 minutes. After washing in PBS containing 0.15% TRITON X-100 surfactant (The Dow Chemical Company, Midland, MI, http://www.dow.com) at room temperature (RT, 24°C) for 15 minutes, sections were incubated with 1% bovine serum albumin (Sigma-Aldrich) at RT for 30 minutes to block nonspecific binding. Sections were then incubated with primary antibody at RT for 1 hour and washed three times in PBS containing 0.15% TRITON X-100 for 15 minutes. Control incubations were conducted with the appropriate normal mouse and rabbit IgG at the same concentration as the primary antibody, and the primary antibody for the respective specimen was omitted. The sections were then incubated with the appropriate secondary antibodies at RT for 1 hour. After being washed three times with PBS, the sections were then coverslipped using glycerol-containing propidium iodide (PI) (Nacalai Tesque, Inc., Kyoto, Japan, https://www.nacalai.co.jp), and examined under a confocal microscope (FluoView; Olympus Corporation, Tokyo, Japan, http://www.olympus.co.jp).

Table 1. Sequences for PCR and shRNA

LGR5 (NM_003667), Forward 5′-GAGGATCTGGTGAGCCTGAGAA-3′
Reverse 5′-CATAAGTGATGCTGGAGCTGGTAA-3′
SHH (NM_000193.2), Forward 5′-ACGGCCCAGGGCACCATTCT-3′
Reverse 5′-GGACTTGACCGCCATGCCCA-3′
Ptch1 (NM_000264.3), Forward 5′-TCGCTCTGGAGCAGATTTCCAAGGG-3′
Reverse 5′-GCAGTCTGGATCGGCCGGATTG-3′
Smo (NM_005631.4), Forward 5′-GTGAGTGGCATTTGTTTTGTGGGC-3′
Reverse 5′-CAGGCATTTCTGCCGGGGCA-3′
Gli1 (NM_005269.2), Forward 5′-GCCCCCATTGCCCACTTGCT-3′
Reverse 5′-TGCAGGGGACTGCAGCTCC-3′
Gli2 (NM_005270.4), Forward 5′-GGCCGCCTAGCATCAGCGAG-3′
Reverse 5′-CACCGCCAGGTTGCCCTGAG-3′
β-Actin (NM_ 001101), Forward 5′-GGACTTCGAGCAAGAGATGG-3′
Reverse 5′-ATCTGCTGGAAGGTGGACAG-3′
sh LGR5, 5′-CCGGGCTCTACTGCAATTTGGACAACTCGAGTTGTCCAAATTGCAGTAGAGCTTTTT-3′
sh NT, 5′-CCGGCAACAAGATGAAGAGCACCAACTCGAGTTGGTGCTCTTCATCTTGTTGTTTTT-3′

Abbreviations: LGR5, leucine-rich repeat G protein-coupled receptor 5; PCR, polymerase chain reaction; Ptch1, protein patched homolog one receptor molecule; SHH, sonic Hedgehog; sh NT, short hairpin nontarget; shRNA, short hairpin RNA; Smo, smoothened receptor molecule.

Real-Time Polymerase Chain Reaction

Real-time polymerase chain reaction (PCR) was performed following our previously described method [19]. To prepare the samples, we first separated the central cornea from the peripheral cornea using an 8-mm trephine. We then stripped the Descemet's membrane including CECs using micro forceps under a microscope to separate the corneal epithelium, stroma, and endothelium in the central and peripheral cornea, respectively. We then separated the corneal epithelial cells from the corneal stroma using dispase treatment (37°C for 1 hour). All samples were homogenized in lysis buffer (Buffer RLT; QIAGEN, Inc., Valencia, CA http://www.qiagen.com) and total RNA was eluted by use of the RNeasy Mini Kit (QIAGEN) according to the manufacturer's instructions. The relative abundance of transcripts was detected by use of SYBR Green PCR Master Mix (Applied Biosystems, Inc., Foster City, CA http://www.appliedbiosystems.com) according to the manufacturer's instructions. The primers that were used are shown in Table 1.

Flow Cytometry

For the cell sorting of $LGR5^{high}$ cells, monkey CECs prepared as described above were passaged in 1:2 dilutions and cultured to subconfluence. The CECs were dissociated to single cells by use of TrypLE Select. We then performed the following two experiments. First, the CECs were fixed in 70% (wt/vol) ethanol at 4°C for 2 hours, washed with PBS, and incubated at RT for 15 minutes with 1% FBS. The CECs were then incubated with 1:100-diluted anti-rabbit LGR5 and 1:100-diluted anti-mouse Ki67, washed, and incubated with 1:1500-diluted Alexa Fluor 488-conjugated goat anti- rabbit IgG (Life Technologies) and 1:1000-diluted Cy3 anti-mouse IgG (Jackson Immunoresearch Laboratories). Flow cytometric analyses were then performed with FACS Aria II (BD Biosciences).

Second, the CECs were washed with PBS, and then incubated at RT for 15 minutes with 1% FBS. They were then incubated with 1:100-diluted anti-rabbit LGR5 at RT for 20 minutes, washed, and incubated with 1:1500-diluted Alexa Fluor 488-conjugated goat anti-rabbit IgG (Life Technologies). $LGR5^{high}$ and $LGR5^{low}$ cells were isolated by use of fluorescence activated cell sorting (FACS) Aria II, and the resultant cells were then cultured on an eight-well chamber slide with poly-L-lysine (Sigma-Aldrich). After 5 days of culture, those cells were immunostained by anti-mouse Ki67 as described above, and the $Ki67^{high}$ cells in each group were then counted ($n = 4$).

Measurement of Cell Area

Each isolated cell fraction was centrifuged and resuspended in culture medium. Cells (approximately 100 cells/ml) were placed in a six-well plate and photographed under an inverted microscope. Cell areas were measured randomly (200 cells/fraction) using Scion Image software and statistically analyzed [23].

RNA Interference

Short hairpin RNA (shRNA) was purchased from Sigma-Aldrich. The *LGR5* shRNA targeted sequences and the nontarget (NT) shRNA sequences are shown in Table 1. The lentivirus plasmid DNA was transfected to the HEK293T cells along plasmid packaging plasmid mixture (MISSION Lentiviral Packaging Mix; Sigma-Aldrich) using a commercially available transfection reagent (FuGENE HD; Roche Diagnostics Corporation, Indianapolis, IN, http://www.roche-diagnostics.com). After 18 hours, the media was aspirated off and replaced with complete medium. The quantity of lentiviral particles was assessed by HIV-1 p24 Antigen ELISA (Zepto-Metrix Corp., Buffalo, NY, http://www.zeptometrix.com) according to the manufacturer's instructions.

Construction of Lentivirus Plasmid Vector for Gene Expression

For the construction of the lentivirus plasmid vector that expresses the introduced gene, *LGR5*, a commercially available lentiviral vector (pLenti6.3_V5-TOPO; Life Technologies) was used. cDNAs were amplified with a primer pair (Forward Primer: CTACTTCGGGCACCA TGGACACCT, Reverse Primer: CACATATTAATTAGAGACATGGGA) encompassing an entire coding sequence of *LGR5*, gel-purified, and then ligated into the lentivirus plasmid vector.

The expression lentivirus Production and Infection were in a modified version of our protocol used for the shRNA [25]. Briefly, the lentivirus plasmid DNA was transfected to the HEK293T cells along with the plasmid packaging plasmid mixture ViraPower Lentiviral Packaging Mix (Life Technologies) which contains pLP1, pLP2, and pLP/VSVG plasmids and FuGENE HD as the transfection reagent. After 18 hours, the media was aspirated off and replaced with complete

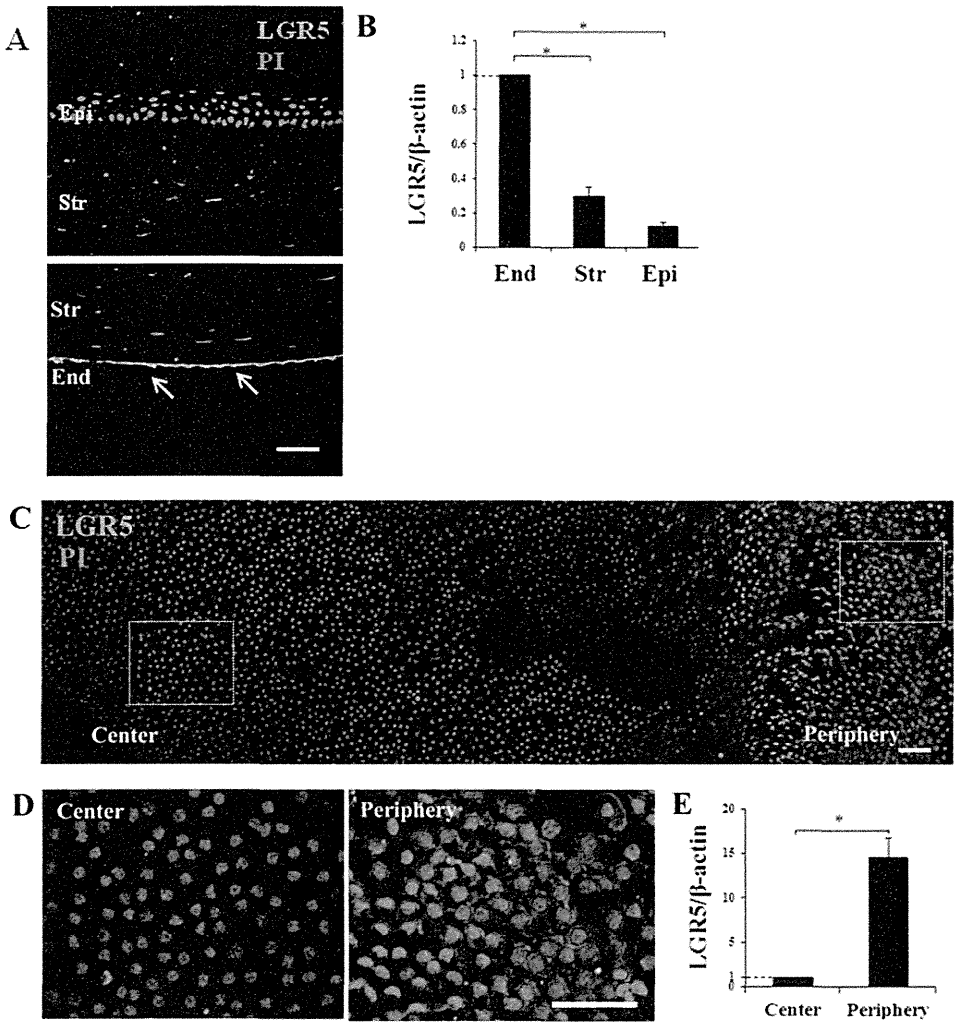

Figure 1. Unique expression pattern of leucine-rich repeat G protein-coupled receptor 5 (LGR5) in human corneal endothelial cells (CECs). **(A):** Immunostaining of LGR5 in a human cornea. Arrows point to CECs. Scale bar = 100 μm. **(B):** Real-time polymerase chain reaction (PCR) for *LGR5* in the cornea. Mean ± SEM. *, $p < .05$. $n = 4$. **(C):** Whole-mount immunostaining of LGR5 in human CECs. Scale bar = 100 μm. **(D):** Higher magnification of boxed areas in **(C)**. Scale bar = 100 μm. **(E):** Real-time PCR for *LGR5* in the central and peripheral CECs. Mean ± SEM. *, $p < .05$. $n = 3$. Abbreviations: LGR5, leucine-rich repeat G protein-coupled receptor 5; PI, propidium iodide.

medium and the quantity of lentiviral particles was then assessed.

Gene Transfer

The culture supernatant containing the infection-competent virus particle was harvested to human CECs at 5,000 cells/well in a six-well plate with FNC Coating Mix for 24 hours (Multiplicity of infection (MOI) = 1) using the culture medium described above. The supernatant was applied onto cultivated CECs in the presence of 4 μg/ml polybrene. As puromycin-resistant colonies (shRNA experiment) and blasticidin-resistant colonies (overexpression model) were collected, cells were cultured in the presence of 0.4 μg/ml of puromycin and 2 μg/ml of blasticidin, with the media being changed every 2 days.

Western Blotting

The cultivated human CECs were washed with PBS and then lysed with lysis buffer containing PBS, 1% TRITON X-100, 0.5 M EDTA, Phosphatase Inhibitor Cocktail two (Sigma-Aldrich), and Protease Inhibitor Cocktail (Roche Diagnostics). Detection of activated β-catenin (nonmembrane bound) was performed according to the previously reported protocol [26]. Briefly, cell lysates treated with Con A Sepharose 4B (GE Healthcare) were incubated at 4°C for 1 hour. After centrifugation at 4°C for 10 minutes, the supernatants were transferred to new tubes and Con A Sepharose was added to each tube and incubated at 4°C for 1 hour. Finally, after a brief centrifugation, the supernatants were transferred to new tubes and their protein concentration was determined.

The proteins were then separated by SDS polyacrylamide gel electrophoresis and transferred to polyvinylidene difluoride membranes. The membranes were then blocked with 1% ECL Advance Blocking Reagent (GE Healthcare) in Tris Buffered Saline with Tween 20 (TBS-T) buffer and were incubated with primary antibody at 4°C overnight. After being washed three times in TBS-T buffer, the polyvinylidene fluoride (PVDF) membranes were incubated with appropriate HRP-conjugated anti-rabbit or mouse IgG secondary antibody at RT for 1 hour. The membranes were exposed by use of the ECL Advance Western Blotting Detection Kit (GE Healthcare), and then examined by use of the LAS-3000 (FujiFilm Corporation, Tokyo, Japan, http://www.fujifilm.com) imaging system.

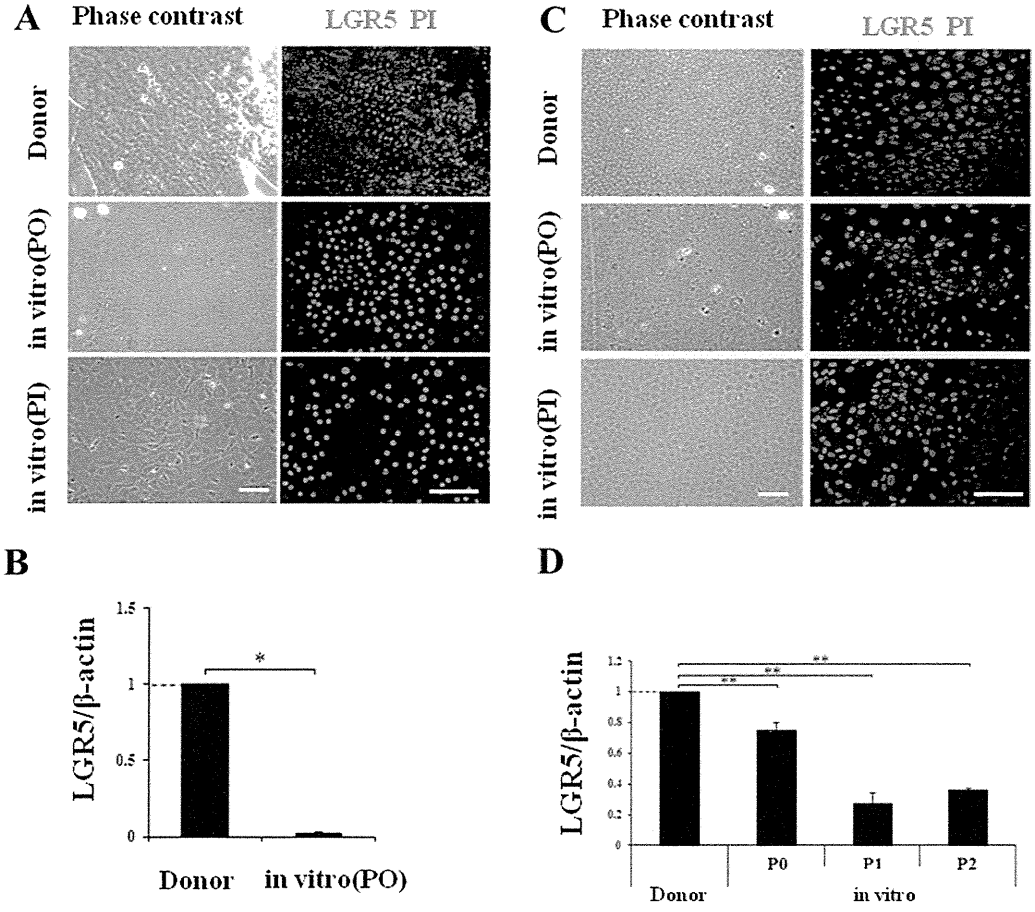

Figure 2. Downregulation of leucine-rich repeat G protein-coupled receptor 5 (LGR5) in cultivated corneal endothelial cells (CECs). **(A):** Phase contrast image and immunostaining of LGR5 in donor and in vitro human CECs. Scale bars = 100 μm. **(B):** Real-time polymerase chain reaction (PCR) for *LGR5* in donor and in vitro human CECs. Mean ± SEM. *, $p < .05$. $n = 4$. **(C):** Phase contrast image and immunostaining of LGR5 in donor and in vitro monkey CECs. Scale bars = 100 μm. **(D):** Real-time PCR for *LGR5* in donor and in vitro monkey CECs. Mean ± SEM. **, $p < .01$. $n = 3$. Abbreviations: LGR5, leucine-rich repeat G protein-coupled receptor 5; PI, propidium iodide; PO, passage 0.

Results

Unique Expression Pattern of LGR5 in Human Donor CECs

The expression pattern of LGR5 in human CECs was investigated by indirect immunofluorescence. On examination of the CECs of those tissues, intensive LGR5 expression was observed, especially in the peripheral area. However, LGR5 was only minimally expressed in the corneal epithelium and stroma (Fig. 1A). Real-time PCR showed that compared with stroma and epithelium, mean *LGR5* messenger RNA (mRNA) expression was significantly upregulated in the CECs (*$p < .05$, $n = 4$, mean age: 60 years) (Fig. 1B). Thus, among the corneal tissues, the expression of LGR5 was found to be most prominent in the CECs.

Next, we examined the location pattern of LGR5 using whole-mount immunofluorescence ($n = 3$, mean age: 64 years). The expression of LGR5 was observed in the peripheral-region CECs, yet its level gradually decreased in CECs located towards the central region (Fig. 1C, 1D). Real-time PCR clearly showed that the expression of *LGR5* in the peripheral regions was upregulated in comparison with the central region (8-mm diameter) (*$p < .05$, $n = 3$, mean age: 70 years) (Fig. 1E). These findings indicate that in corneal tissue, LGR5 is uniquely expressed in the peripheral CECs.

Downregulation of LGR5 in In Vitro Culture Conditions

It is well known that the proliferative potential of CECs varies among species [27]. To date, it is extremely difficult to consistently culture human CECs which retain a healthy morphology and high cell density. In contrast, we previously reported that under the proper in vitro conditions, monkey and rabbit CECs can proliferate reasonably well [2, 20–22]. Thus, to gain an insight into the molecular mechanism that underlies the varying proliferative potentials of CECs, we examined the expression of LGR5 in vitro.

Phase contrast microscopy photographs of human peripheral donor CECs revealed that they exhibited a confluent monolayer of smaller-size homogeneously hexagonal cells (Fig. 2A). In contrast, cultured CECs (P0, P1) were found to be enlarged and not homogeneously hexagonal (Fig. 2A). Immunostaining showed that LGR5 was well-expressed in the peripheral donor CECs (Fig. 2A). Worthy of note, the expression of LGR5 was only minimally observed in the cultured CECs in vitro (P0, P1) (Fig. 2A). Real-time PCR showed that the mean *LGR5* mRNA expression was significantly downregulated in in vitro CECs as compared to that in peripheral donor CECs (*$p < .05$) (Fig. 2B).

Phase contrast photographs of monkey CECs showed that both the peripheral donor and the in vitro (P0, P1) cells exhibited a confluent monolayer of smaller-size

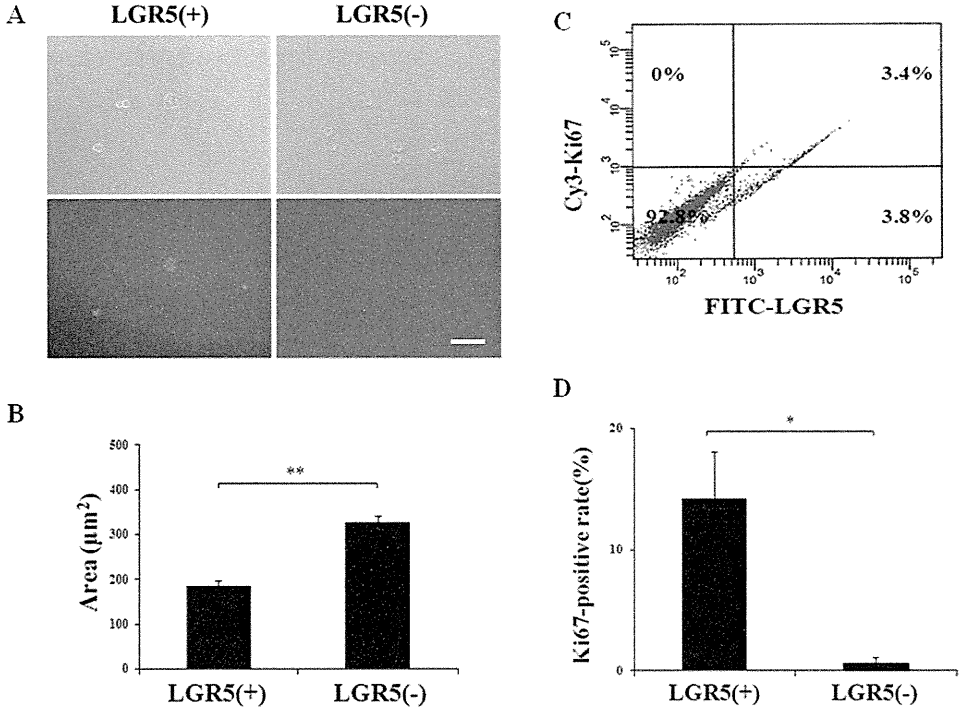

Figure 3. Characterization of leucine-rich repeat G protein-coupled receptor 5 (LGR5$^+$) Monkey corneal endothelial cells. **(A):** Phase contrast image and immunocytochemistry for LGR5 in LGR5$^+$ cells and LGR5(−) cells after cell sorting. Scale bar = 100 μm. **(B):** Average cell size of LGR5$^+$ (184.6 ± 45.8 μm^2) and LGR5$^-$ (326.78 ± 78.8 μm^2). Mean ± SEM. **, $p < .01$. $n = 35$. **(C):** Cell proliferation of LGR5$^+$ by double-immunostaining. LGR5$^+$/Ki67$^+$; 3.4%, LGR5$^+$/Ki67$^-$; 3.8%, LGR5$^-$/Ki67$^+$; 0%, LGR5$^-$/Ki67$^-$; 92.8%. **(D):** Ki67-positive rate of LGR5$^+$ and LGR5$^-$. Mean ± SEM. *, $p < .05$. $n = 4$. Abbreviations: FITC, fluorescein isothiocyanate, LGR5, leucine-rich repeat G protein-coupled receptor 5.

homogeneously hexagonal cells (Fig. 2C). The expression pattern of LGR5 in the monkey CECs closely mimicked that of in the human donor CECs (data not shown). Immunostaining of those cells showed that LGR5 is moderately expressed both in the donor cells and in vitro cells (Fig. 2C), even though the mean *LGR5* mRNA expression in vitro gradually decreased through the cell passages (*$p < .05$) (Fig. 2D). In view of these findings using human and monkey cells, it is likely that LGR5 may play a role in maintaining the cell integrity of CECs.

LGR5$^+$ CECs Were Small and Exhibited Higher Proliferative Potential

To examine the characteristics of the LGR5$^+$ and LGR5$^-$ cell fractions, the subsets were isolated by flow cytometry. To validate the cell sorting procedure, immunofluorescence for LGR5 confirmed its expression at the protein level in the purified fraction (Fig. 3A).

As the highest clonogenicity is reportedly found in the smallest keratinocytes [28], the cell size in each isolated fraction was measured by use of Scion Image software. Viewed under an inverted microscope, the LGR5$^+$ cells were found to be clearly smaller than the LGR5$^-$ cells (Fig. 3B), and the average size of the LGR5$^+$ cells was significantly smaller than that of the LGR5$^-$ cells (184.6 ± 45.8 μm^2 vs. 326.78 ± 78.8 μm^2, respectively, $n = 35$, **$p < .01$).

Next, to assess the cell-cycling status of each isolated cell fraction, FACS was used for double-staining with LGR5 and Ki67. FACS analysis showed that the LGR5^{high}/Ki67^{high} cell fraction was 3.4%, whereas the LGR5^{high}/Ki67^{low} cell fraction was 3.8% (Fig. 3C). Most interestingly, all LGR5^{low} cell fractions showed the Ki67 low level (92.8%). To further examine the proliferative capacity of each isolated cell fraction in detail, isolated cell fractions were cultivated on cell chamber slides. Five days later in culture, the percentage of Ki67-labeled cells in the LGR5$^+$ and LGR5$^-$ cells was 14.2 ± 3.87% and 0.58 ± 0.5%, respectively, rendering the difference in the Ki67-labeling index statistically significant (*$p < .05$) (Fig. 3D), suggesting that without the LGR5 expression, CECs do not have proliferative ability.

Active HH Signaling Induced LGR5 Expression

HH signaling reportedly plays a key role in various kinds of biological processes, such as cell differentiation, proliferation, and growth [16, 29, 30]. To define the properties of LGR5 in CECs at the molecular level, we first examined the expression of HH signaling-related molecules in human donor CECs. Of interest, the levels of *SHH*, *Gli1*, and *Gli2* mRNA were found to be elevated in CECs located in the peripheral-region as compared to those in the central region (Fig. 4A). On the other hand, the expression level of smoothened (*Smo*) and protein patched homolog one (*Ptch1*) receptor molecules in the HH pathway was similar (Fig. 4A). Thus, HH signaling was clearly activated in the peripheral-region CECs, suggesting that a regional variation of HH signaling activity does exist.

To determine whether the expression of LGR5 in the CECs was regulated by the HH signaling pathway, the peripheral donor CECs (outside the 8-mm central cornea area) were incubated in culture medium (Dulbecco's modified Eagle's medium + 5% FBS) and stimulated using recombinant SHH (an HH ligand, 100 ng/ml), purmorphamine (an HH agonist, 2 μM) [31], and cyclopamine (an HH antagonist, 2 μM) [32] for 24 hours at 37°C in 5% CO_2. As expected, expression of *LGR5* in the peripheral-region CECs, yet not in the central-region CECs, was found to be upregulated by SHH and

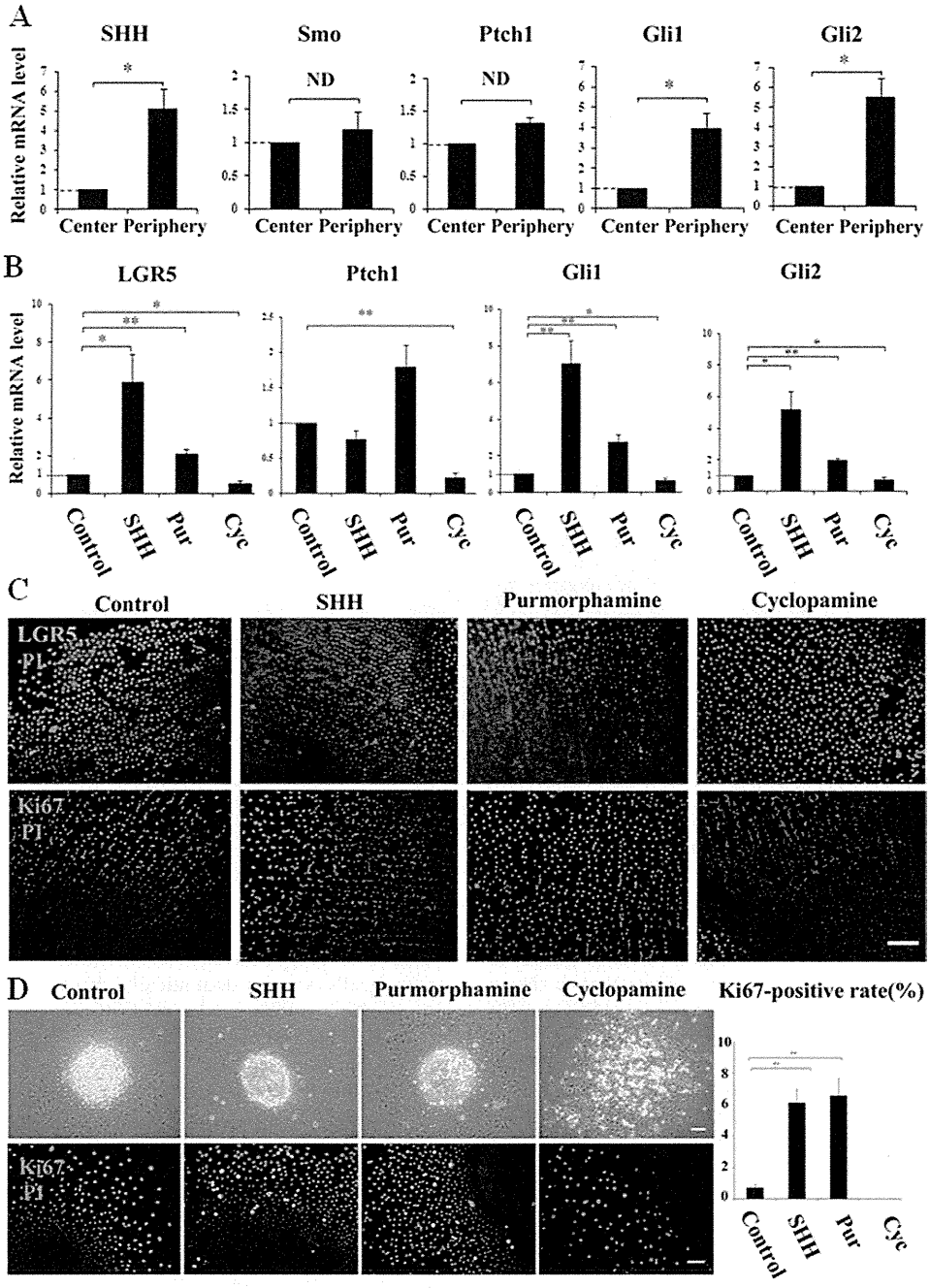

Figure 4. Hedgehog (HH) signaling pathway in corneal endothelial cells (CECs). **(A):** Real-time polymerase chain reaction (PCR) for HH signal-associated genes (*SHH*, *Smo*, *Ptch1*, *Gli1*, and *Gli2*) in central and peripheral human donor CECs. Mean ± SEM. *, $p < .05$. $n = 4$. **(B):** Real-time PCR of leucine-rich repeat G protein-coupled receptor 5 (*LGR5*), *Ptch1*, *Gli1*, and *Gli2* in human donor CECs treated with SHH, purmorphamine (Pur), and cyclopamine (Cyc), respectively. Mean ± SEM. *, $p < .05$; **, $p < .01$. $n = 4$. **(C):** Immunostaining of LGR5 and Ki67 in human donor CECs treated with SHH, Pur, and Cyc, respectively. Control: 0.1% dimethyl sulfoxide (DMSO). Scale bar = 100 μm. **(D):** Immunostaining of Ki67 in cultivated human CECs treated with SHH, Pur, and Cyc, respectively. Control: 0.01% DMSO. Scale bar = 100 μm. Ki67-positive rate of human CECs treated with SHH, Pur, and Cyc, respectively. Mean ± SEM. **, $p < .01$. $n = 5$. Abbreviations: LGR5, leucine-rich repeat G protein-coupled receptor 5; mRNA, messenger RNA; ND, No significant difference; PI, propidium iodide; SHH, sonic Hedgehog.

purmorphamine stimulation, whereas *LGR5* expression was reduced by cyclopamine stimulation at both the mRNA and protein levels (Fig. 4B, 4C). The expression patterns of *Gli1* and *Gli2* were similar to that of *LGR5*, but HH activation did not dramatically have an influence on *Ptch1*, the HH receptor (Fig. 4B).

Next, immunohistochemistry for Ki67 was performed to elucidate whether or not the HH pathway induced donor CEC proliferation. As human CECs are mitotically inactive and show weak-to-no proliferative capacity *in vivo* [3], an elevated expression of Ki67 was not observed in all experimental groups, suggesting that stimulation of the HH pathway alone is not sufficient to induce donor CEC proliferation (Fig. 4C). However, CECs reportedly retain the capacity to proliferate in vitro [4], so we investigated whether the HH pathway induced CEC proliferation in vitro. The expression of Ki67 was found

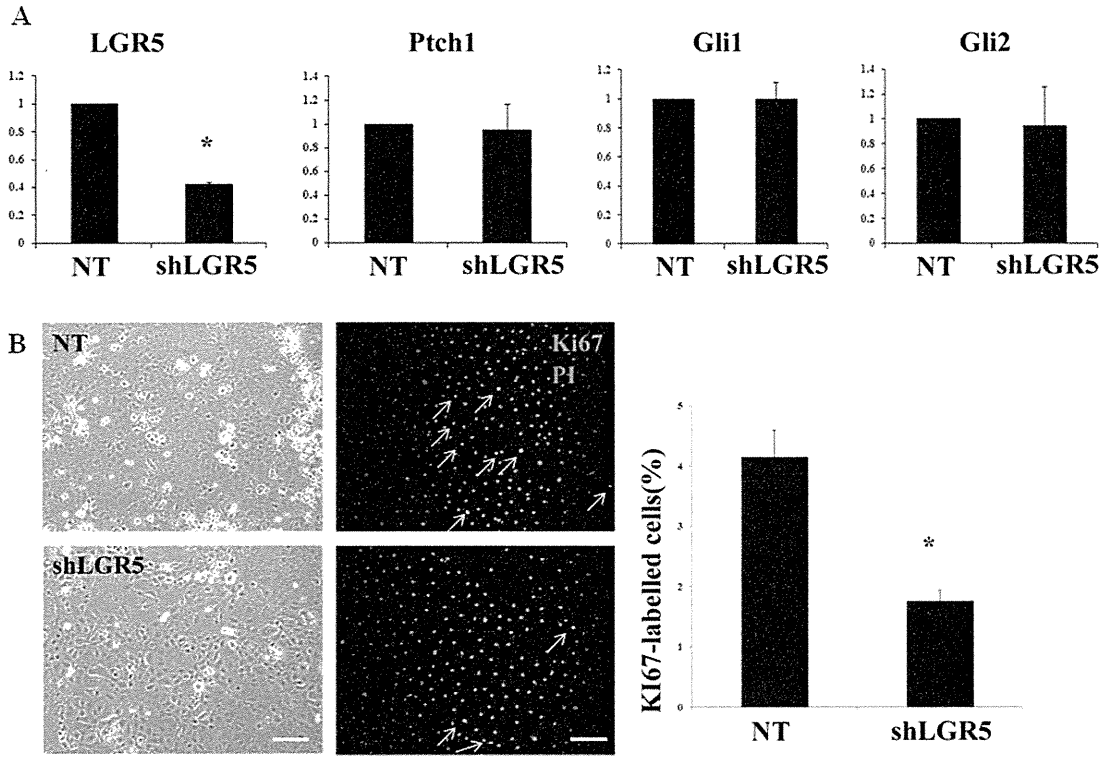

Figure 5. Effect of short hairpin *LGR5* (shLGR5) in human corneal endothelial cells (CECs). **(A):** Real-time polymerase chain reaction for leucine-rich repeat G protein-coupled receptor 5 (*LGR5*), *Ptch1*, *Gli1*, and *Gli2* in nontarget (NT)- and shLGR5-transfected cells. Mean ± SEM. *, $p < .05$. $n = 3$. **(B):** Phase contrast microscopy image and immunostaining of Ki67 in NT- and shLGR5-transfected human CECs. Arrows point to $Ki67^+$ cells. Scale bar = 100 μm. Mean ± SEM. *, $p < .05$. $n = 5$. Abbreviations: LGR5, leucine-rich repeat G protein-coupled receptor 5; NT, nontarget; PI, propidium iodide; shLGR5, short hairpin LGR5.

to be upregulated in response to SHH- and purmorphamine-stimulation, however, it was not upregulated in response to cyclopamine (Fig. 4D). These findings indicate that in the in vitro situation, the HH pathway is able to induce CEC proliferation. We posit that CECs treated with cyclopamine were unable to maintain their normal hexagonal morphology (Fig. 4D). Furthermore, Real-time PCR showed that the expression of *LGR5* in the cultured CECs with SHH stimulation was elevated as compared to those without SHH stimulation. Immunohistochemistry showed that after SHH stimulation, the expression of LGR5 in the cultured CECs was elevated in some of the cells, yet not in all of the cells (supplemental online Fig. 1). In view of these findings, we discovered for the first time that LGR5 is the target molecule of HH signaling in CECs and that CEC maintenance is partially regulated by the HH pathway.

Downregulation of LGR5 Decreased the Proliferation of CECs

The direct effect of LGR5 on the CECs was elucidated by the knockdown of *LGR5* by shRNA. For this experiment, primate cultivated CECs were used, due to the fact that cultured human CECs rarely express LGR5 (Fig. 2A, 2B). Nine sets of shRNA were designed, and the efficacy of their knockdown potential was then examined. Of those, shRNA-589 was found to be the most effective for knocking down the *LGR5* mRNA expression (approximately 60% knockdown) (Fig. 5A). Real-time PCR for *Ptch1, Gli1, and Gli2* showed that no significant differences were found between the short hairpin *LGR5* (shLGR5) group and the control (Fig. 5A). To demonstrate the effect of knocking down the *LGR5* gene on CEC proliferation, immunocytochemistry for Ki67 was performed. Compared with the control, cell morphology of the shLGR5-treated cells was not dramatically changed, however, the number of $Ki67^+$ cells in the shLGR5-treated cells was greatly reduced (Fig. 5B). These findings indicated that downregulation of *LGR5* did not have an effect on the HH pathway, but did decrease CEC proliferation in vitro.

Persistent *LGR5* Expression Inhibited MT Through the Wnt Pathway

To investigate the direct effects of persistent *LGR5* expression on CECs, we attempted to overexpress LGR5 using lentivirus containing CMV-*LGR5*- mRFP. In this experiment, human cultivated CECs (fourth passage, 62-year-old donor) were used, as they rarely express LGR5 (Fig. 2A). Real-time PCR showed that the expression of *LGR5* in *LGR5*-transfected cells (6 days after transfection) was about 60 times higher than that in NT vector-transfected cells ($p < .01$) (Fig. 6B). Immunofluorescence was used to confirm that the expression of *LGR5* in the LGR5-transfected cells was elevated in comparison with that in the NT cells (Fig. 6A). Of great interest, the relative mRNA levels of the HH signaling molecules in *LGR5*-transfected cells were downregulated as compared to those in the NT cells (Fig. 6B), indicating that LGR5 operates as a negative feedback regulator of the HH pathway.

Human CECs are reportedly vulnerable to morphological fibroblastic change under normal culture conditions [5]. To better demonstrate the effect of persistent *LGR5* expression, we used fourth-passaged cultivated CECs. After lentivirus transfection, some of the NT cells still exhibited an enlarged and elongated shape (fibroblastic change) (Fig. 6A). Of great

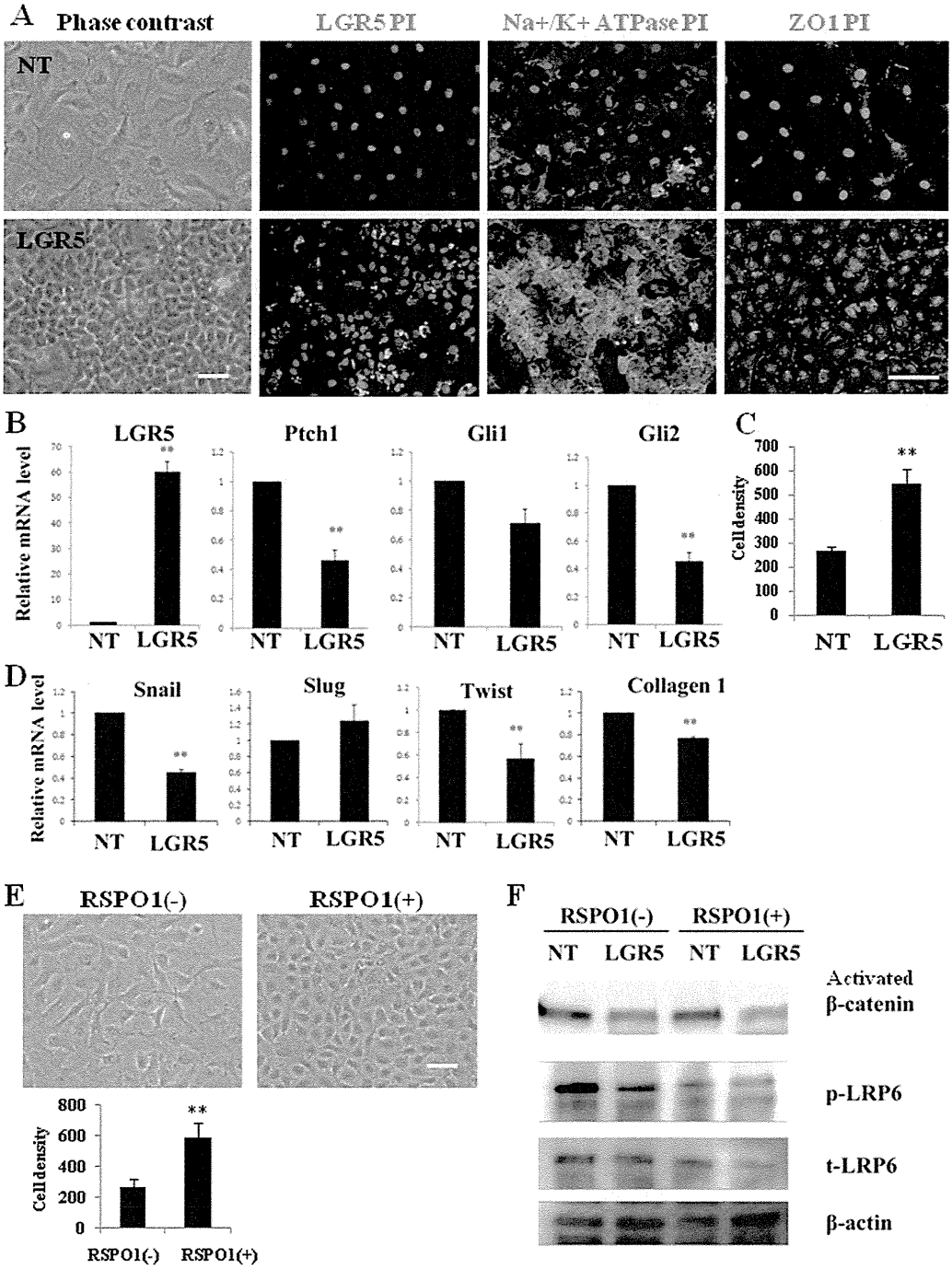

Figure 6. Function of leucine-rich repeat G protein-coupled receptor 5 (LGR5) and R-spondin-1 (RSPO1) in corneal endothelial cells (CECs). **(A):** Phase contrast microscopy image and immunostaining of LGR5, Na+/K+ ATPase, and ZO1 in nontarget (NT)- and *LGR5*-transfected human CECs. Scale bar = 100 μm. **(B):** Relative expression of *LGR5, Ptch1, Gli1, and Gli2* messenger RNA in NT- and *LGR5*-transfected cells. Mean ± SEM. **, $p < .01$. $n = 3$. **(C):** Cell density of NT- and *LGR5*-transfected cells. Mean ± SEM. **, $p < .01$. $n = 5$. **(D):** Real-time polymerase chain reaction for EMT-associated genes (*Snail, Slug, Twist, and collagen1*) in NT- and *LGR5*-transfected cells. Mean ± SEM. **, $p < .01$. $n = 3$. **(E):** Phase contrast image of human cultivated CECs with or without RSPO1 (50 ng/ml). Scale bar = 100 μm. Cell density of CECs with or without RSPO1. Mean ± SEM. **, $p < .01$. $n = 5$. **(F):** Western blotting of activated β-catenin, pLRP6, tLRP6, and β-actin in NT- and LGR5-transfected cells with or without RSPO1 (50 ng/ml). Abbreviations: LGR5, leucine-rich repeat G protein-coupled receptor 5; mRNA, messenger RNA; NT, nontarget; PI, propidium iodide; RSPO, R-spondin-1.

interest, the *LGR5*-transfected cells gradually changed their morphology and were shown to be compact, smaller-size, homogeneously hexagonal cells, resuming the normal physiological morphology (Fig. 6A). Cell density of the *LGR5*-transfected cells was found to be greatly elevated compared with that of the NT cells (Fig. 6C). To examine the function of cultivated CECs transfected with the NT and *LGR5* vector, immunohistochemistry was performed for Na^+/K^+ ATPase and ZO1. The expression of these two functional proteins was found to be much greater in the *LGR5*-transfected cells than in the NT cells, even though these expression patterns were not typical in comparison with those in in vivo CECs (Fig.